MURINE EMBRYONIC STEM CELLS AND HYPOXIA: GROWTH KINETICS, METABOLISM, AND PLATING EFFICIENCY

by

Daryl St. Laurent

B.S. Chemical Engineering
Massachusetts Institute of Technology

Submitted to the Biological Engineering Division in
partial fulfillment of the requirements for the degree of

Master of Engineering in Biomedical Engineering
at the
Massachusetts Institute of Technology

June 2004

Signature of Author: _____
Biological Engineering Division
March 19, 2004

Certified by: _____
Jean-François P. Hamel
Lecturer, Associate Industrial Liaison
Thesis Supervisor

Accepted by: _____
Roger D. Kamm
Professor of Biological Engineering and Mechanical Engineering
MEBE Graduate Program Director

Accepted by: _____
Alan J. Grodzinsky
Professor of Electrical, Mechanical, and Biological Engineering
Director, Center for Biomedical Engineering
Chairman, Biological Engineering Graduate Program

MURINE EMBRYONIC STEM CELLS AND HYPOXIA: GROWTH KINETICS, METABOLISM, AND PLATING EFFICIENCY

by
Daryl St. Laurent
Submitted to the Biological Engineering Division on March 19, 2004
in partial fulfillment of the requirements for the degree of
Master of Engineering in Biomedical Engineering

ABSTRACT

There is reason to believe that embryonic stem cells would grow favorably in a hypoxic environment. These cells come from the pre-implantation embryo, whose native environment is the hypoxic mammalian reproductive tract. Growing stem cells in an environment with higher oxygen levels (i.e. the atmospheric oxygen levels that are normally used to cultivate stem cells) could be bad for the cells, as oxygen is toxic due to its powerful oxidative capacity. In this experiment, J1 murine embryonic stem cells were grown at 0%, 2%, 5%, 10%, and 20% oxygen by volume to assess the effects that lower oxygen levels have on stem cell growth, plating efficiency, and metabolism. Two reaction vessels were built so that the cells could be grown in a controlled environment. Premixed gas cylinders were used to flush the vessels and an optical probe was used to measure the headspace oxygen concentration. Cells were found to grow faster than atmospheric conditions when in a moderately hypoxic environment where the oxygen concentration was between 2% and 10%, and considerably slower than atmospheric conditions as the headspace oxygen concentration approached zero. Maximum cell density decreased, glucose-lactate yield increased, glucose-cell yield decreased, and glutamine-cell yield decreased as headspace oxygen decreased. There were no strong correlations between oxygen concentration and glutamine-ammonia yield or plating efficiency. From the results of this study, it appears that it may be preferable to grow murine embryonic stem cells in a moderately hypoxic environment around 10% oxygen to increase the growth rate while minimizing the maximum cell density and metabolic inefficiency compromises.

Thesis Supervisor: Jean-François P. Hamel

Title: Associate Industrial Liaison, Lecturer

ACKNOWLEDGEMENTS

I have been lucky to have had the support of many helpful and supportive people throughout my time as a graduate student. I would like to thank Manny Otero, Ryo Ohashi, and Mike Previte for their guidance through the planning stages of my thesis work. The three of them taught me what I know about cell culture, and challenged me to think critically. Professor Bevin Engelward has been amazingly helpful throughout my research with her knowledge of stem cells and with her biological perspective. I would also like to thank Yas Hashimura for being a great research companion and source of entertainment. Finally, I would like to thank my advisor, Jean-François Hamel, for his guidance when I needed help, and for giving me the opportunity to think and work independently. Working in this manner has allowed me to grow as a researcher and a scholar.

Last, and by no means least, I would like to thank the people who were a source of moral support throughout my work as a graduate student. My family has been amazingly supportive throughout all the ups and downs of the program, and they have been wonderfully understanding when I got bogged down with work and disappeared. I would also like to thank my best friend, Francesca. When times got tough, she was always there to listen and calm me down. I wouldn't have been able to make it through without everyone's help, and I have been very lucky to work with so many wonderful people.

Polestar Technologies, Inc (Needham Heights, MA) generously provided the optical oxygen probe used for this study. This work was supported in part by the Engineering Research Centers Program of the National Science Foundation under NSF Award EEC 9843342, and by the MIT department of Chemical Engineering.

TABLE OF CONTENTS

LIST OF TABLES

LIST OF FIGURES

Nomenclature

BHK Baby Hamster Kidney

CHO Chinese Hamster Ovary

DMEM Dulbecco's Modified Eagle Medium

DMSO Dimethylsulfoxide

EDTA Ethylenediaminetetraacetic Acid

ESC Embryonic Stem Cell

LIF Leukemia Inhibitory Factor

ROS Reactive Oxygen Species

TCA Tricarboxylic Acid

Chapter 1

1 Introduction

Embryonic stem cells are an exciting topic in modern biology. These "master cells" have the ability to develop into any of the cells of an organism. Because of this powerful ability, stem cells have potential for applications in embryology, pharmacology, toxicology, and as a powerful source for cell and tissue therapy. (Wobus, 2001)

1.1 Embryonic Stem Cells

Stem cells are unspecialized cells that have the ability to differentiate into the wide range of specialized cell types that make up the body. With proper stimulus, they can be grown indefinitely in an undifferentiated state while maintaining their ability to differentiate in the absence of stimulus. Current research involves two types of stem cells: adult stem cells and embryonic stem cells (ESC). Adult stem cells are present in fully grown organisms and are less specialized than embryonic stem cells. They are unipotent, in that they can only develop into a subset of the cells of the body. Adult stem cells are found in tissues, and have the ability to develop into the various cells that make up the tissue. For instance, hematopoieitc stem cells are adult stem cells that generate various different blood cells. No adult stem cells have yet been isolated that are capable of differentiating into every possible cell type. (*Stem Cells*, 2001)

In contrast to adult stem cells, embryonic stem cells are pluripotent, meaning they have the ability to develop into any type of cell found in the body. (*Stem Cells*, 2001) However, embryonic stem cells lack the totipotent ability of the fertilized egg because they cannot form the trophectoderm. (Smith, 2001) This limitation arises from the origin of stem cells: the inner cell mass of an embryonic blastocyst (Martin, 1981; Evans & Kaufman, 1981). Formation of the blastocyst is the last stage of embryonic development before implantation occurs. (*Stem Cells*, 2001) After fertilization, the mouse zygote divides until it becomes a 16-cell morula. At this point, the totipotent cells of the embryo specialize into one of two types. The outer cells become the trophectoderm, and the inner cells become the inner cell mass. The morula then develops into a spherical blastocyst (Figure 1-1), which is characterized by an outer layer of flat trophoectoderm cells, a lump of round cells that make up the inner cell

mass, and a fluid filled cavity called the blastocoel. The trophoectoderm will eventually develop into the chorion, which will connect the fetus to the mother so nutrients can reach the developing organism. The inner cell mass, which is the source of embryonic stem cells, will ultimately develop into all the tissues of the embryo. (Gilbert, 1997)

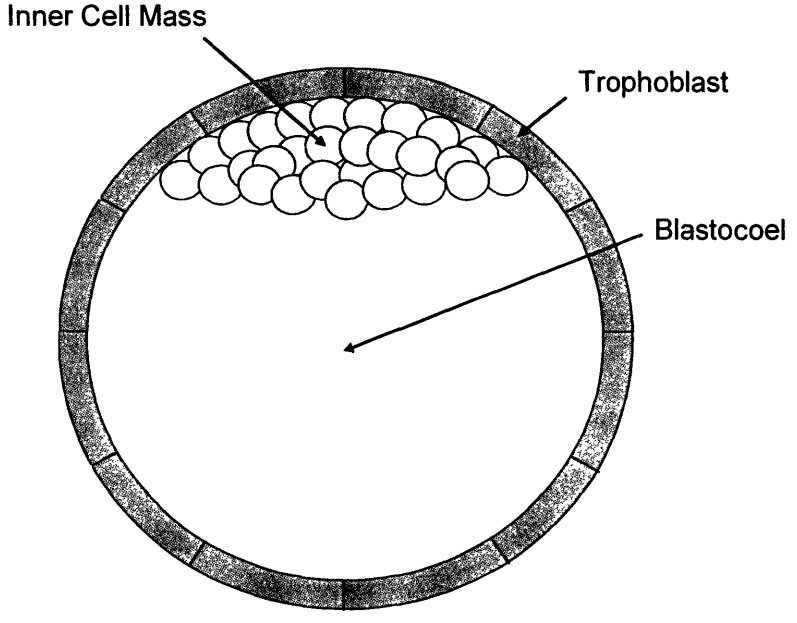

Figure 1-1: Diagram of a blastocyst cross-section. A flat layer of trophoectoderm cells form a fluid-filled cavity called the blastocoel. Embryonic stem cells come from the inner cell mass, which is made of a cluster of round cells.

Embryonic stem cells have a number of defining characteristics. The most important ones for the purposes of the research presented in this document are long-term growth in an undifferentiated state (Smith, 2001) while maintaining pluripotency (Bradley, Evans, Kaufman, & Robertson, 1984); ability to develop into cells from endoderm, ectoderm, and mesoderm embryonic germ layers (Bradley et. al., 1984); clonogenic ability (Smith, 2001); and lack of a G1 checkpoint (Savatier, Lapillonne, Grunsven, Rudkin, & Samarut, 1995). Long term growth ability is useful from an engineering perspective because it allows cells to be grown in large quantities and still have them be viable stem cells. Pluripotency is valuable because of its potential therapeutic applications. Such applications include tissue replacement therapy, studying early human development, drug testing, and toxicity studies. (Nichols 2001) Because stem cells are clonogenic, all offspring are identical, which lends itself well to genetic

manipulation. A gene can be added to the stem cell, and all daughter cells will contain the recombinant gene product. Because stem cells lack a G1 checkpoint and do not need any kind of signal to enter the S phase, they spend most of their time synthesizing DNA. As a result, approximately 75% of embryonic stem cells *in vitro* are found in the S phase (Savatier et. al., 1995). This in turn means that stem cells grow rapidly.

A photograph of the J1 murine embryonic stem cells used in this study can be seen in Figure 1-2. When in suspension (after being treated with trypsin), J1 cells have diameters between 15 μm and 20 μm.

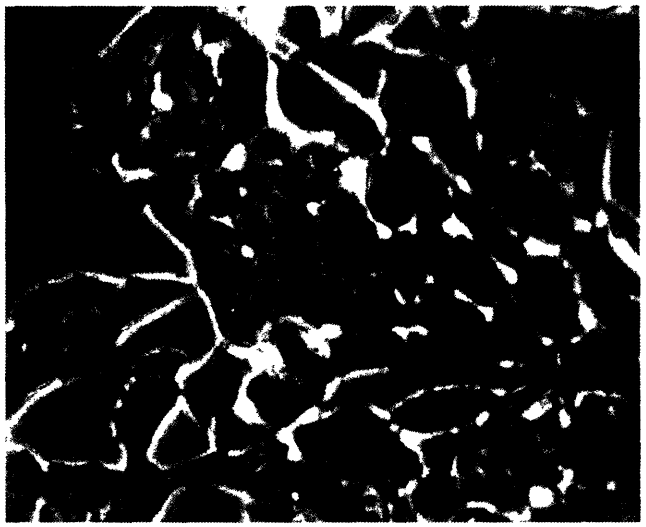

Figure 1-2: J1 embryonic stem cells. The photograph is of cells growing on a tissue culture plate. Photo was taken with a Fuji FinePix 4700 zoom digital camera through an Olympus CK2 microscope at a magnification of 200x. Image was digitally enhanced to improve contrast.

Embryonic stem cells naturally differentiate into embryoid bodies, and stimulus is required to keep them in an undifferentiated state. One means to keep them in the undifferentiated state is through the use of feeder cells (Evans & Kaufman, 1981). A simpler approach is to use purified recombinant leukemia inhibitory factor (LIF) to maintain ESC. Cells cultured with LIF have been shown to keep their pluripotency and can be used to form a chimaeric mouse (Williams et. al., 1988).

1.2 Cell Metabolism

A summary of some relevant metabolic pathways occurring in stem cells can be seen in Figure 1-3. Of particular interest are the fates of the two major fuel sources in cell culture medium: glucose (which is converted to lactate, in part) and glutamine (which is oxidized to carbon dioxide). Both can interchangeably be used for energy sources. Glucose is also essential for anabolic reactions (H. Zielke, C. Zielke, & Ozand 1984). Glutamine is a key amino acid because it is consumed at an order of magnitude higher rate than other amino acids (Wang, Yang, Huzel, and Butler, 2002).

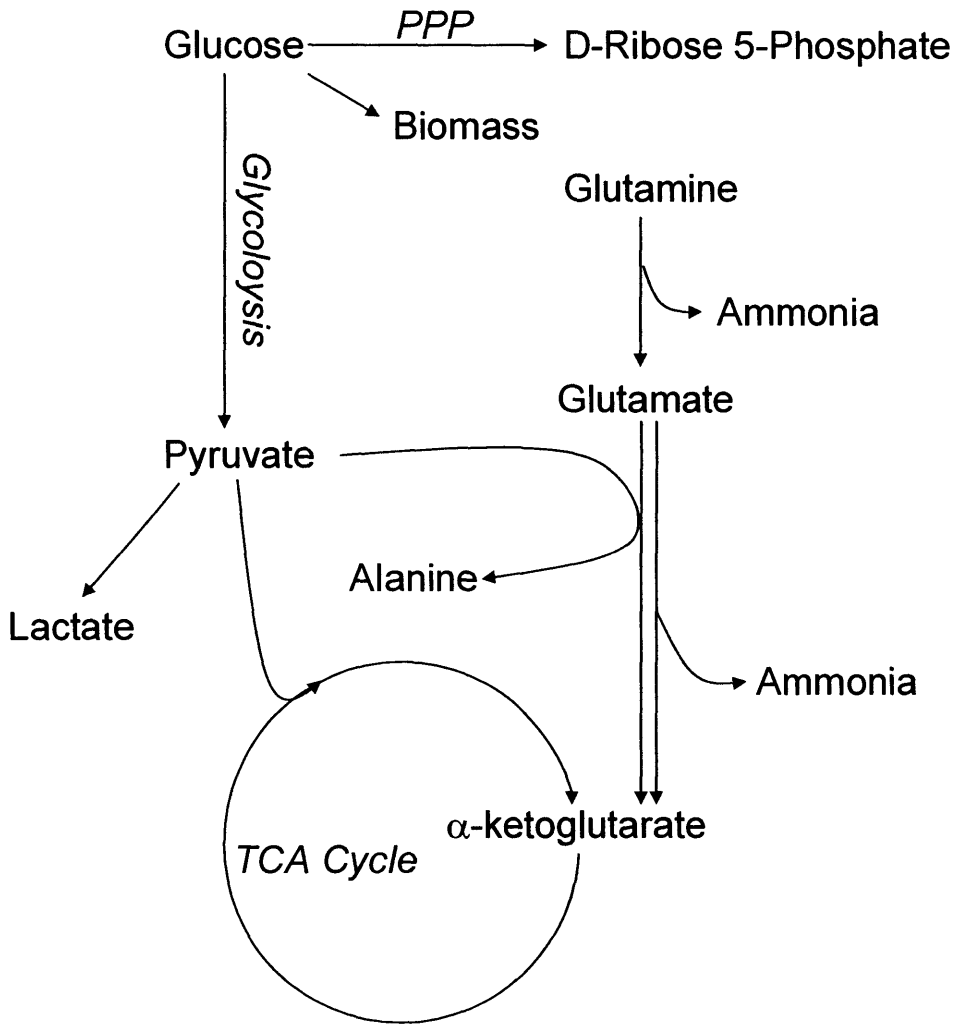

Figure 1-3: Summary of important metabolic processes. The two major food sources for stem cells are glucose and glutamine, and the two major waste products are lactate and ammonia. PPP: Pentose Phosphate Pathway. TCA: Tricarboxylic Acid.

Glucose has three primary fates: pyruvate, production of biomass, and the pentose-phosphate pathway. Pyruvate can then either be converted into lactate, enter the tricarboxylic acid (TCA) cycle, or—in cases of metabolic overflow—be converted to alanine. Glutamine can be used to produce other amino acids, or incorporated into biomass, but the majority is converted to glutamate. Glutamate can then be converted to α-ketoglutarate and enter the TCA cycle via one of two pathways: a less efficient pathway (glutamate:pyruvate transaminase) involving the production of alanine, and a pathway (glutamate dehydrogenase) that results in the production of an additional molecule of ammonia (Cruz, Moreira, & Carrondo 1999). Ammonia is an important metabolite because it is toxic to cells at high concentrations (Cruz, Freitas, Alves, Moreira, & Carrondo, 2000). Fortunately for the health of cells, ammonia evaporates from medium (Lao & Toth, 1997). A summary of the various possible end products of glutamine metabolism can be seen below in Table 1-1.

Metabolite	% of Glutamine Metabolism
Alanine	55.
Aspartate	3.2
Glutamate	3.8
Lactate	8.7
CO_2	22.
Intracellular Protein	7.2
Extracellular Protein	0.24

Table 1-1: End products of glutamine metabolism in hybridoma cells (Petch & Butler, 1994)

It is important to note that lactate can be produced as an end product of glutamine metabolism (Zielke et. al., 1980) as well as glucose metabolism.

A summary of literature values for various important yields can be seen in Table 1-2.

Cell Line	$Y_{Lac/Glc}$ (mol/mol)	$Y_{Amm/Gln}$ (mol/mol)	$Y_{Nt/Glc}$ (10^9 cells/mmol)	$Y_{Nt/Gln}$ (10^9 cells/mmol)
Hybridoma	1.5 [1] 1.45 [2]	0.75 [1] 0.82 [2]	0.29 [2]	0.46 [2]
CHO	1.5–1.6 [3]	0.7 [3]	N/A	N/A
BHK	1.6 [4] 1.5 [5]	0.65 [4] 0.7–0.9 [5]	0.2 [4]	0.6 [4]

Table 1-2: Literature values for yields. Yields are given for cells grown in medium with high glucose and glutamine concentrations. No cell-glucose or cell-glutamine yields were found for CHO cells.

1: Zhou, Rehm, Europa, & Hu, 1997
2: Ljunggren & Hägström, 1995
3: Lao & Toth, 1997
4 Linz, Zeng, Wagner, & Deckwer 1997
5 Cruz, Freitas, Alves, Moreira, & Carrondo 1999

1.3 Hypoxia

In vivo, embryos grow in hypoxic conditions. In hamsters and rabbits, the blastocyst grows in oxygen levels that are considerably lower than atmospheric concentrations with respective oxygen levels at 5.3% and 3.5% by volume. The concentration is even lower in the monkey uterus at 1.5% O_2 (Fisher & Bavister, 1993). Oxygen levels during the first few days of rat pseudopregnancy were found to be between 3% and 5% (Yochim & Mitchell 1968). Mouse blastocysts were found to grow best when *in vitro* oxygen concentration was between 2.5% and 5%. (Quinn & Harlow, 1978) Embryos likely grow better in hypoxic conditions (Cannigia et. al., 2000) than in atmospheric conditions because of the lower levels of free radicals. Superoxide radicals have been shown to inhibit development of mouse embryos. At atmospheric conditions, 500 mg/mL of superoxide dismutase, a free radical scavenger, was shown to increase blastulation rate tenfold over the control culture without scavengers (Noda et. al., 1991). There are several ways to lower the concentration of reactive oxygen species (ROS), including addition of catalase, superoxide dismutase, and ethylenediaminetetraacetic acid (EDTA). However, the most practical method to protect developing mouse embryos seems to be lowering the oxygen tension to 5%, which has been shown to improve development (Orsi & Leese, 2001). The presence of oxygen gradients embryos are essential for activating certain genes (Adelman, Gertsenstien, Naggy, Simon, & Maltepe, 2000). Furthermore, plating efficiency has been shown to be higher in hypoxic conditions. (Wiles, 1993; Potocnik, Nielsen, & Eichmann, 1994; Gassmann et. al., 1996).

Prior studies have been done with several cell lines growing in hypoxic conditions. A greater conversion of glucose to lactate with decreasing oxygen concentration was seen in myocytes

(Silverman, Wei, Haigney, Ocampo, & Stern, 1997), hybridoma (Ozturk & Palsson, 1990; Europa, Gambhir, Fu, & Hu, 2000), and murine embryonic cells (Sanford, Westfall, & Jackson, 1970). However, it may be possible to have an environment that is too hypoxic for adequate cell growth, as it has been shown that ESC grow more slowly when the oxygen level drops below 2% than they do at oxygen levels above 2% (Iyer et. al., 1998; Carmeliet et. al., 1998). Hybridoma cells have been adapted to grow in apoxic conditions provided that the adaptation is sufficiently slow (Ozturk & Palsson, 1990), so it may be possible to do the same with ESC.

1.4 Cellular Growth Kinetics

A general equation for viable cell growth is given by Jang and Barford (2000):

$$\frac{dX_V}{dt} = \mu X_V - \mu_D X_V - \frac{F_O}{V} X_V \qquad \text{(Eq. 1-1)}$$

Since no cells were removed from the plate until it was removed from the incubator for sampling, the third term can be ignored. X_V is equal to the viable cell mass, μ is the specific growth rate, and μ_d is the specific death rate. Dividing by the average mass of a cell yields:

$$\frac{dN_V}{dt} = (\mu - \mu_D) N_V \qquad \text{(Eq. 1-2)}$$

Analysis in this experiment was done over the exponential growth phase of the cell life cycle, so it was assumed that μ and μ_D were constant. Assuming that the death rate is much smaller than the growth rate, μ - μ_D can be combined into a single parameter μ, giving the equation that was used for analysis of growth kinetics:

$$\frac{dN_V}{dt} = \mu N_V \qquad \text{(Eq. 1-3)}$$

Integrating and rearranging gives:

$$\ln N_V = \ln N_o + \mu t \qquad \text{(Eq. 1-4)}$$

The growth rate can be found by fitting growth data to (Eq. 1-4). Equations used for linear regression are listed in Appendix A.1 and A.2. Doubling time can then be found by manipulating (Eq. 1-4):

$$\ln \frac{N_V}{N_o} = \ln 2 = \mu t_d \Rightarrow t_d = \frac{\ln 2}{\mu} \qquad \text{(Eq. 1-5)}$$

1.5 Calculating yields

An apparent yield (Lao & Toth, 1997) is given by:

$$Y_{produced/consumed}(mol/mol) = \frac{mol\ of\ product\ produced}{mol\ of\ product\ consumed} \qquad \text{(Eq. 1-6)}$$

If the metabolite consumed is x and the metabolite produced is y, (Eq. 1-6) is equivalent to:

$$Y_{y/x} = -\frac{\Delta y}{\Delta x} \qquad \text{(Eq. 1-7)}$$

Although the total changes in metabolite concentrations could be used, it is more rigorous to perform a linear regression with the metabolite concentrations to calculate the yield (which is equivalent to the slope of the regression line).

Chapter 2

2 Materials and Methods

A series of experiments were set up to test the hypothesis that hypoxic conditions would be more favorable for growing murine embryonic stem than the normoxic conditions in incubators currently used for the majority of stem cell culture.

2.1 Research Objectives and Experimental Design

Three sets of experiments were done to test the hypothesis that hypoxic conditions are more favorable than normoxic conditions for culture of murine embryonic stem cells. The experiments were a control culture grown in normal incubator conditions, a set of experiments to measure plating efficiency as a function of oxygen concentration, and a set of experiments to measure metabolic yields and cellular growth kinetics as a function of oxygen concentration.

2.1.1 Incubator Control

As a control, cells were cultured in "normal" humidified incubator conditions at 95% air and 5% CO_2. Glucose, lactate, and viable cell concentration were measured as a function of time, and were used to determine the doubling time and glucose-lactate yield of J1 cells growing in an incubator. Cells were grown in 6-well plates, and samples were taken every six hours. These data were used to determine over what time points cells grew exponentially. This region of exponential growth was used as a guide for planning future metabolism and kinetics experiments, as it is desirable to have as many cell concentration data points as possible in the exponential growth phase of the cell life cycle to make accurate doubling time calculations.

2.1.2 Plating Efficiency

Previous studies have shown that a hypoxic environment increases the plating efficiency of embryonic stem cells (Wiles, 1993; Potocnik, Nielsen, & Eichman 1994; Gassmann et. al., 1996). A second set of experiments was done to determine if this trend is reproducible. Three 6 cm plates were seeded with approximately 100 cells and placed together in the small reaction vessel. The headspace oxygen concentration was maintained at either 0%, 2%, 5%, 10%, or 20% oxygen for one day so the cells would attach to the surface of the plate at a controlled

oxygen concentration. The number of colonies that were formed were used to calculate the plating efficiency. The experiment was repeated to see if the trends were reproducible.

2.1.3 Metabolism and Kinetics

Two sets of experiments were done to study the cellular growth kinetics and metabolism of J1 embryonic stem cells in five different oxygen concentrations: 0%, 2%, 5%, 10%, and 20%. The first run was done to establish trends in the data. A second run was done to verify whether the trends were reproducible. Fifteen plates were grown in the large reaction vessel under controlled oxygen concentrations. Cell concentration was measured as a function of time, as were pH and glucose, lactate, glutamine, ammonia, and glutamate concentrations. A clear vinyl lid was used for the first run, and a clear Lexan® lid was used for the second run. A discussion of why the lid was different for the second run can be seen in section 3.4.

2.2 Oxygen-Controlled Cell Culture Reactors

Two reactors were built so cells could be grown in a controlled environment. The smaller reactor was designed to hold either one 10cm plate, or a 6-well plate. The larger reactor was designed to hold sixteen 6cm plates. A photograph of the smaller reactor can be seen in Figure 2-1.

Figure 2-2 depicts the setup used to control the gas composition of the reactor. A gas tank containing a mixture of CO_2, O_2 and N_2 was connected to a rotameter (AALBORG 032-41T) so flow through the reactor could be controlled. Gas coming out of the rotameter was fed into a filter flask where it was bubbled through water to humidify it. The gas was then filtered before it passed into the reactor. A filter was placed on the outlet so contaminated air could not pass backwards into the reactor when it was not in use. A second filter flask was used for some of the runs so that its bubbles were visual evidence of gas passing through the reactor. The reactor and filter flasks were placed inside a Juan IG-150 CO_2 incubator so the environment was kept at 37°C. Temperature was measured with a beaded type K thermocouple and a VWR dual-channel digital thermometer, and was shown to not vary by more than 0.5°C. The small reactor was in the center of the incubator, and the large reactor was placed in the center of the bottom tray.

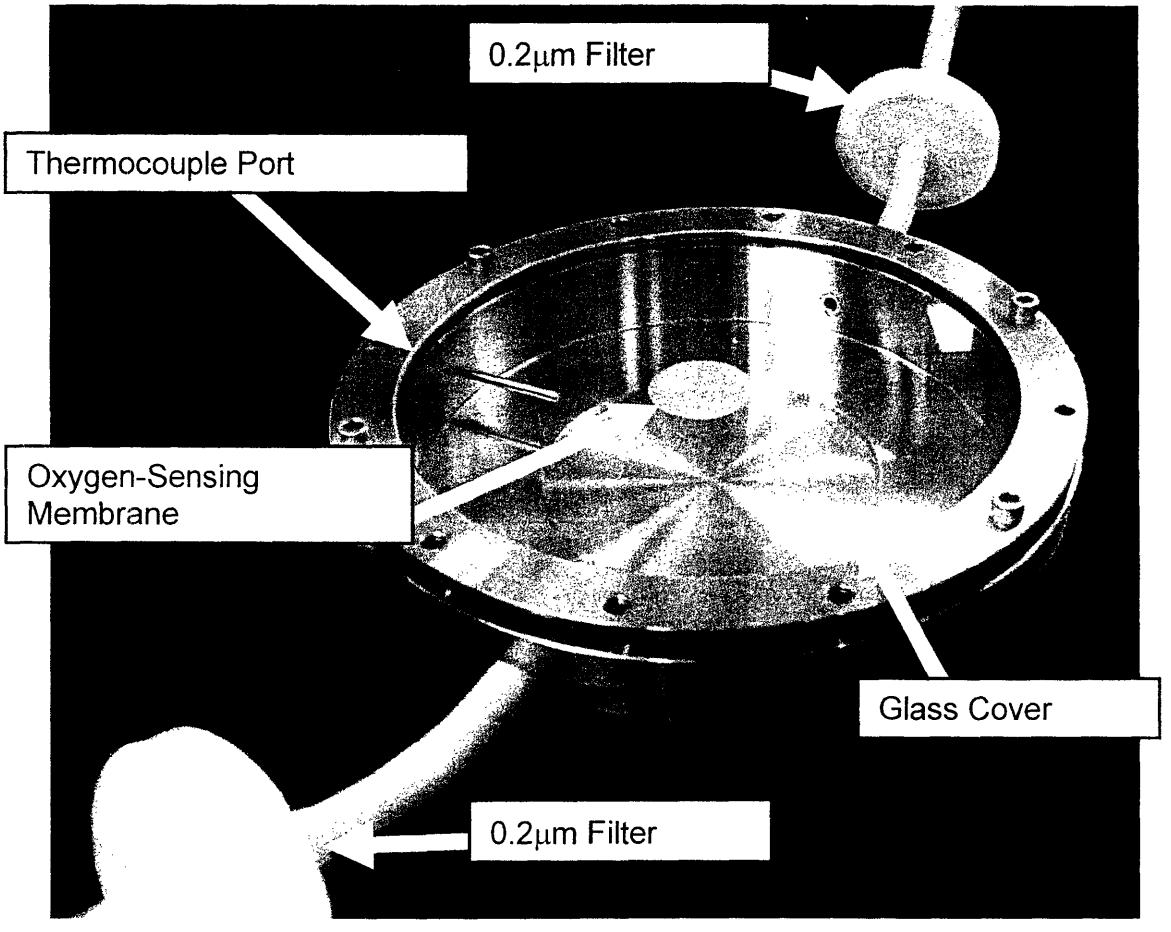

Figure 2-1: Small reactor. Reactor consists of a chamber made of 316L stainless steel, a glass cover, and a lid that is bolted down to hold the glass in place. The underside of the glass has a Polestar oxygen sensing membrane adhered to it. A thermocouple port protrudes into the space so temperature measurements can be made. Inlet and outlet gas lines (Masterflex 6402-25) have 0.2 μm filters to help prevent contamination. Inner diameter of the reaction chamber is 15.4 cm and 36 cm and the chamber depth is 2.4 cm and 2 cm for the small and large chamber, respectively.

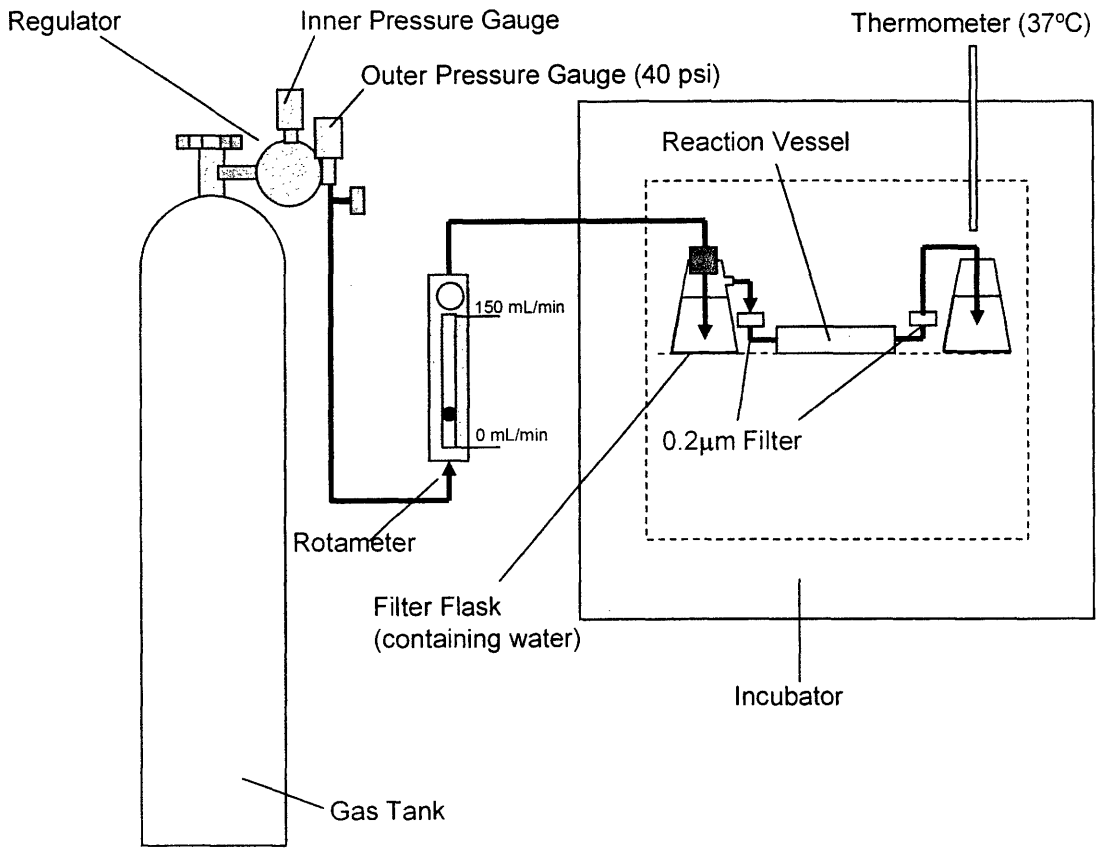

Figure 2-2: Reactor setup. A gas tank containing a mixture of 5% CO_2, either 0%, 2%, 5%, 10%, or 20% O_2, and the balance nitrogen was connected to a regulator such that the outlet pressure was 40 psi. The gas tank fed an Aalborg rotameter that had a scale from 0 to 150 cc/min. The rotameter was calibrated with an Alltech 7080 Portable Direct Reading Flow Check. Air coming out of the rotameter was bubbled through water, filtered with a 0.2 µm filter, and passed through the reaction vessel. A second filter was placed in the outlet stream to prevent contamination from moving backwards into the reactor when air was not being passed through. The gas was finally bubbled through water so that there was visual evidence that gas was passing through the reactor. The reaction vessel was placed inside a Juan IG-150 CO_2 incubator.

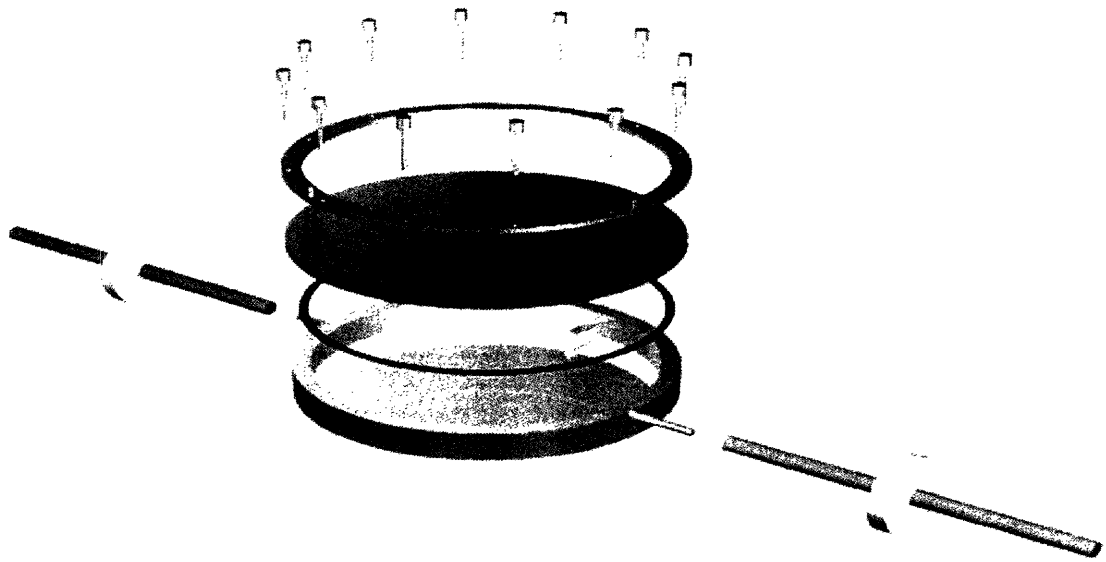

Figure 2-3: Exploded view of reactor. Drawing is not to scale, but is intended to show how the different parts fit together. The main body of the reactor is the round dish at the bottom center of the schematic. Rubber tubing (Masterflex 6402-25 Norprene) was connected to the inlet and outlet vents. Filters (0.2 μm) were placed in the gas lines. A capped cylinder protrudes into the body of the reactor for temperature measurements with a thermocouple. A rubber o-ring was used to make a seal between the top of the reaction chamber and the glass, Lexan®, or vinyl placed on top. Bolts were used to secure the lid and seal the chamber.

Figure 2-3 depicts the reactor construction. The body of the reactor was made of autoclavable 316L stainless steel and contained a round chamber, an inlet vent, an outlet vent, and a capped thermocouple port. Tubing connected the vents to 0.2 μm filters. An o-ring was placed between the top of the reactor and the lid to create a seal. The lid was made of glass in the small reactor, and Lexan® plastic (GE Plastics) in the large reactor. An oxygen-sensing membrane was placed on the underside of the lid. In the large reactor, the lid was bolted directly to the reactor. In the small reactor, a disc was placed on top of the glass, and was bolted to the reactor to hold the glass in place. Twelve evenly spaced bolts were used to secure the reactor lids. For many of the runs, fewer bolts were used (usually six) so that the cells would spend less time outside the incubator. Both reactors were autoclaved at 250 °F for 30 minutes prior to their first use, and wiped down with ethanol before each experiment. They were only opened inside the biosafety cabinet except for the convective evaporation study.

2.3 Gases

Four hypoxic gas concentrations were chosen: 0%, 2%, 5%, and 10% O_2. The control was 20% O_2. Each tank had 5% CO_2 to regulate the pH of the Dulbecco's Modified Eagle Medium (DMEM) carbonic acid buffer. The balance of each tank was made up of N_2. There were minor variations in gas concentration from tank to tank, but these variations were less than the variations observed due to how well the reactor was sealed (whether the o-ring was flat or round, how well the o-ring sealed with the lid, and how much the bolts were tightened). To simplify the results, the oxygen concentrations reported are the target concentrations. The measured values sometimes deviated a few percent from the reported values, and the ranges over which this deviation occurred are tabulated in Table 3-4. The range of concentrations for each value did not overlap, so they were neglected for the purposes of the analysis, with the understanding that trends were more important than predicting the behavior at a precise gas concentration.

2.4 Measuring Headspace Oxygen

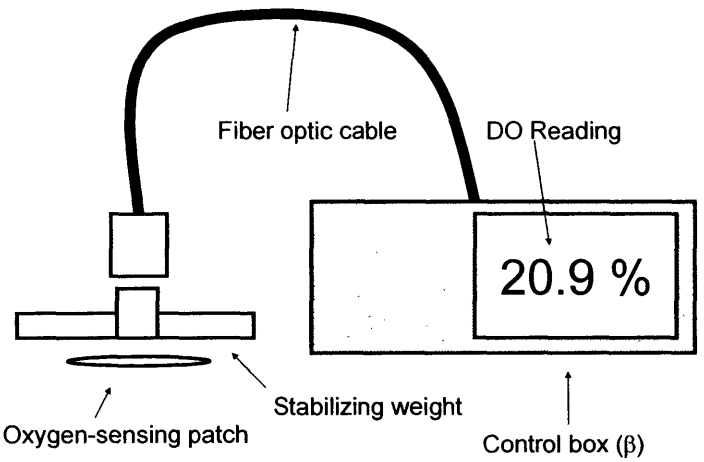

Figure 2-4: The Polestar oxygen probe

Headspace oxygen was measured by an optical probe borrowed from Polestar Technologies (Figure 2-4). A fiber optic cable was connected to a weight so that it would point to the patch on the underside of the lid. The other end of the cable was connected to the control box that displayed the current headspace oxygen concentration. The probe measures oxygen by bouncing light off an oxygen-sensitive patch (approximately 1 inch in diameter) placed on the

underside of the reactor lid. The oxygen concentration is a function of the temperature and the phase shift of the light that bounces back. The probe was used to verify the hypoxic state of the reactor, and a VWR dual-channel digital thermometer with a type K thermocouple was used to check the temperature inside the reactor to validate the probe reading.

2.5 Cell Culture

Stem Cells used in the work described were of the J1 cell line. A large batch of low-passage number cells was frozen down prior to starting experimental work. Vials of cells were thawed periodically during the experiments. (See 2.5.4: Thawing Stem Cells) Experiments were started with cells that had been growing for no more than two weeks after being thawed. Cells were discarded after this point. "Warm" reagents have been heated to 37°C in a water bath. Fresh medium (and LIF) was used to feed stem cells every day unless otherwise indicated. (See 2.5.3: Feeding Stem Cells) Frozen stem cells were stored at -140°C for long-term storage, or no longer than 1 month at -80°C for short-term storage. A ThermoForma (Waltham, MA) 360 Series Steri-Cycle incubator incubator was used for cell culture, and a Jouan Inc. (Winchester, VA) IG-150 CO2 incubator was used for the reactor.

LIF used was prepared by Ryo Ohashi. It was produced as a LIF-GEX fusion protein in the JM109 strain of *E. coli*, and purified via affinity chromatography using glutathione beads. The fusion protein was digested with thrombin, and the concentration was determined by visually comparing cells growing in the recombinant LIF with cells growing in commercial LIF of known concentration. It was determined that 2 μL of LIF was needed for each mL of medium.

2.5.1 Stem Cell Medium

Stem cells were cultured in Dulbecco's Modified Eagle Medium (Gibco 11960-044) supplemented with 2 mM L-glutamine (Gibco 25030-081), 0.1 mM 2-mercaptoethanol (Gibco 21985-023), 1 mM sodium pyruvate (Gibco 11360-070), 0.1 mM non-essential amino acids (Gibco 11140-050), and 15% by volume fetal bovine serum (Hyclone SH30071.03 Lot ANA18039). Leukemia Inhibitory Factor was added to prevent cell differentiation at 0.2% by volume.

2.5.2 Stem Cell Passage

Gelatin solution (1g/L) was added to a tissue culture plate, and the plate was incubated for at least one hour at 37 °C. An appropriate amount of gelatin solution was added the target plate: 5 mL to 10 cm tissue culture plates (BD #353003), 2 mL to 6 cm tissue culture plates (Corning #430166), and 1 mL to each well of a 6-well tissue culture plate (BD #353224). Medium was suctioned off of a confluent 10 cm tissue culture plate, and 2 mL of pre-warmed trypsin-EDTA (Gibco 25200-072) was added. Trypsin was swirled around the bottom of the plate to coat the entire surface, and the plate was returned to the 37 °C incubator for 10 minutes. At least 2 mL of warm stem cell medium was added (more was sometimes added depending on the experiment) to the trypsinized cells, and the mixture was used to wash the bottom of the plate. The pipet was used to mix the cell suspension and break up any clumps. Cell density was counted with a 0.1 mm deep Improved Neubauer hemacytometer, and the trypan blue exclusion method. Excess gelatin was suctioned off the target plate. For a 10 cm plate, approximately $1x10^6$ to $2x10^6$ cells were added to the new plate if the cells were to be ready in two days, and $1x10^7$ cells if the cells were to be ready the next day. An appropriate amount of medium was added to the plate to bring the volume up to 10 mL, and 20 µL of LIF was added. The plate was swirled to disperse the cells evenly, and the plate was returned to the incubator. The procedure was scaled up or down depending on the area of the plates. For a 6 cm plate, 40% of the volumes used for a 10 cm plate were used. For a 6-well plate, 20% of the volumes used for a 10 cm plate were used.

2.5.3 Feeding Stem Cells

Medium was removed from the plate with a Pasteur pipet and a vacuum. An amount of warm medium equal to the volume of medium removed was added to the plate, and 0.2% recombinant LIF by volume was added.

2.5.4 Thawing Stem Cells

Stem cell medium (9 mL) and 20 mL LIF was added to a gelatinized 10 cm tissue culture plate, and the plate was placed in a 37 °C incubator to keep it warm. A cryogenic vial of stem cells was removed from the freezer, and thawed in a 37 °C water bath until it was about half thawed. The gelatinized plate was removed from the incubator, and 1 mL of the mixture was

used to resuspend the contents of the cryogenic vial. The entire contents of the vial were then added to the tissue culture plate, and the plate was returned to the incubator. Medium was changed the following day to remove residual dimethylsulfoxide (DMSO).

2.5.5 Freezing Stem Cells

Freezing medium was prepared by mixing 4 mL stem cell medium, 0.5mL DMSO (CAS 67-68-5) to modify the freezing point, and 0.5 mL fetal bovine serum (Hyclone SH30071.03 Lot ANA18039). Cells were trypsinized as per the stem cell passage protocol. Stem cell medium (8 mL) was used to rinse each plate and bring the total volume up to 10 mL. The contents of the plates were transferred to a centrifuge tube, and a 100 mL sample was taken for counting. The suspension was spun down for 5 minutes, and the cells were counted with the trypan blue exclusion method and a 0.1 mm deep Improved Neubauer hemacytometer. Supernatant was removed after centrifuging, and cells were resuspended at $1x10^7$ cell/mL in freezing medium. 0.6 mL of suspension was added to each cryogenic vial, and the vials were placed in ice for 10 minutes. Vials were then packed with paper towels and placed in a Styrofoam box. The box was frozen at -80 °C overnight, and the vials were transferred to a -140 °C freezer for long-term storage.

2.6 Experimental Procedures

2.6.1 Plating Efficiency: Preparation

To measure plating efficiency, about 100 cells were seeded in each of three 6cm tissue culture plates, and were allowed to form colonies.

Two milliliters of gelatin solution (1g/L) was added to each of three 6 cm tissue culture plates (Corning 430166) and incubated for 1 hour at 37 °C. The remainder of the protocol was done while the gelatin was setting. Two milliliters of pre-warmed trypsin-EDTA (Gibco 25200-072) was added to a confluent 10 cm tissue culture plate and the plates were incubated for 10 minutes at 37°C. After removing the trypsinized plate from the incubator, 8mL of warm stem cell medium was added to wash the bottom of the plate and bring the volume in the plate to 10mL. The contents of the plate were mixed well and transferred to a 15mL centrifuge tube. Centrifuge tubes were used in this procedure only for storing cells. No centrifuging was done.

A 1 mL sample was taken for automated cell counting with an Innovatis Cedex automated cell counting machine. Four serial dilutions were done in which 1 mL of suspension was diluted in approximately 9 mL of medium to bring the cell density to approximately 100 cells/mL. The volume that the suspension was mixed with was adjusted such that the cell density after four dilutions would be about 100 cells/mL. Care was taken to mix the cells thoroughly with a 1 mL micropipette to insure a single cell suspension. The tissue culture plates were removed from the incubator, and the gelatin solution was aspirated off the plates with a Pasteur pipet. Three milliliters of warm medium, 1 mL of serially diluted suspension, and 80 μL of LIF were added to each plate. The inside of the small reaction vessel was wiped with ethanol, and the plates were placed inside the reactor without lids. The reaction vessel was placed in the incubator, and purged with gas at a rotameter (AALBORG 032-41T) flow rate of 145 mL/min for 10 minutes. Gas flow rate was then turned down for 15 mL/min for the remainder of the run. The original sample (used to seed the serial dilutions) was counted 5 times with the trypan blue dye exclusion method using a 0.1 mm deep Improved Neubauer hemacytometer under an Olympus CK2 microscope. The first three measurements were taken with 0.1 mm Reichert Improved Neubauer hemactyometers, and the final two measurements were taken with a 0.100 mm Hausser Scientific Improved Neubauer hemacytometer. Photographs were taken with a Fuji FinePix 4700 zoom digital camera for later counting to minimize the amount of time the cells were left out of the incubator. Headspace oxygen in the reaction vessel was measured periodically using the Polestar® oxygen sensor.

2.6.2 Plating Efficiency: Growing Colonies

After seeding cells and placing them in the reaction vessel, they were allowed to grow in the defined gas concentration overnight. Occasional measurements were taken of the headspace oxygen using the Polestar optical probe to verify that the headspace oxygen concentration remained more or less constant over the course of the run. The maximum and minimum values reached during each run are tabulated in Table 3-4. The next day, the plates were removed from the reaction vessel, and placed in a 37 °C incubator, where the colonies were allowed to grow for 1 week. Medium in the plates was changed every day. Between 2 and 3 mL of medium was used to feed the cells in each plate, and an appropriate amount of LIF (2 μL/mL) was added to keep the cells in the undifferentiated state.

2.6.3 *Plating Efficiency: Counting Colonies*

After the cells had been allowed to grow for one week, the medium was aspirated off the plates, the plates were placed in a dry 37 °C incubator overnight to dry, and the plates were set aside at room temperature until the staining procedure was done. To stain the colonies, 1.5 mL of fixative (3:1 ethanol : acetic acid) was added to each dry plate, and the plates were incubated for 15 minutes at 37 °C. The fixative was aspirated off, and the plates were placed in a 37 °C incubator for 1 hour and allowed to dry. Two milliliters of Crystal Violet stain was added to each plate, and they were incubated for 3 to 4 hours at 37 °C. The stain was then removed with a pipet, and the plates were rinsed by immersing them in a bucket of water. The (now purple) colonies were then counted. Since about 100 cells were seeded per plate, the number of colonies was approximately equal to the plating efficiency. (Plating efficiencies reported were equal to the number of colonies divided by the number of cells seeded.)

2.6.4 *Metabolism/Kinetics: Setup*

Two milliliters of gelatin was added to each of 15 plates, and they were incubated for one hour. Medium and LIF was pre-mixed and kept warm in the 37 °C water bath. After the hour of incubation, the excess gelatin was removed with suction and a Pasteur pipet, and 3.75 mL of medium was added to each plate with a repeating pipette. Plates were then returned to the incubator to keep them warm. A confluent 10 cm plate of cells was trypsinized for 10 minutes at 37°C with 1 mL of trypsin. One milliliter of warm medium was then added to neutralize the trypsin. Cells were mixed thoroughly by repeatedly drawing them up into the pipette and returning them to the plate, and a 100 µL sample was taken for hemacytometer counting. Approximately $4x10^5$ cells were seeded per plate with a repeating pipette. Plates were placed in the large reaction vessel, and the vessel was sealed and placed in the incubator. The vessel was flushed for 20 minutes at a gas flow rate of 250 mL/min. Gas flow was then reduced to 40 mL/min for the remainder of the run.

2.6.5 *Metabolism/Kinetics: Sampling*

The medium was carefully removed from the each plate with a Pasteur pipette and set aside. The samples were then used for glucose and lactate concentration analysis with the YSI 2700 select. Three vials containing 0.5 mL of medium were frozen for later analysis (0.5 mL for YSI

glutamine-glutamate analysis, and 0.5 mL for analysis with a Nova Bioprofiler). One vial of 0.5 mL was refrigerated for later HPLC analysis of pyruvate concentration. The remainder was used to measure the pH of the medium. Cells were then trypsinized for 10 minutes at 37°C with 1 mL of Trypsin-EDTA. One milliliter of medium was added to neutralize the trypsin, and the cell density was measured with the Innovatis Cedex.

2.6.6 Medium Evaporation

The weight of plates was measured using a Mettler AE 163 analytical balance (Mettler-Toledo, Columbus, OH). 6-well plates were stored in a ThermoForma (Waltham, MA) 360 Series Steri-Cycle humidified incubator set to 5% CO_2 and 37°C. 6cm plates were kept either in the incubator, or in the large reaction vessel. Gelatin used had a concentration of 1g/L in water. To prevent static interaction between the plastic plates and the balance tray, a 100 mL glass beaker was placed between the balance and the plate. The balance was tared with the beaker on it.

2.6.6.1 6-Well, 10cm, and 4cm Evaporation

The measurements for 6-Well, 10cm, and 6cm Evaporation were done by Jiovani Visaya. Six 6-well plates (BD #353224), six 6 cm plates (Corning #430166), and six 10 cm plates (BD #353003) were gelatinized with 2 mL of gelatin per well, 5 mL of gelatin, and 10 mL of gelatin (respectively) for 1 hour at 37°C. Gelatin was removed and an amount of medium at 37 °C equal to the amount of gelatin removed was added to each plate. All plates were stored in consistent incubator locations throughout the study. Weight was recorded periodically to determine the evaporation rate.

2.6.6.2 6-Well Medium Evaporation: 3 Wells

Gelatin was added to 3 wells in each of six 6-well plates (BD #353224), and the plates were incubated for one hour. Gelatin was then removed from each well, and the empty weight of each plate was recorded. 2 mL of medium at 37 °C was added to each well, and the mass of each plate with medium was recorded. Plates were placed in a humidified 37 °C incubator in specific locations. Plates were removed periodically, weighed, and returned to the same

positions in the incubator. Linear regression was done to determine the evaporation rate of each plate.

2.6.7 Convective Medium Evaporation

Two milliliters of gelatin was added to each of fifteen 6 cm TC dishes (Corning #430166) and they were incubated at 37 °C for 1 hour. Excess gelatin was removed, and about 4mL of medium was added to each plate. Since the experiment was carried out before new medium componets arrived, the medium used for the evaporation study contained expired non-essential amino acids (expired 2 months prior to the experiment) and sodium pyruvate (expired 3 months prior to the experiment). It was assumed that a small amount of amino acid and pyruvate degradation would not have an appreciable affect the evaporation rate. Plates were weighted before and after the medium was added. Medium added to the plates was cold (approximately 4 °C). The 15 plates were arranged (see Figure 2-5) in the large reaction vessel, and the vessel was sealed and placed in the incubator. The 10% O2 gas mixture was sparged through the vessel for 20 minutes at a flow rate of 250 mL/min, and then the gas flow was turned down to 40 mL/min for the remainder of the run. Pressure going into the rotameter was initially set at 40psi, but one of the gas lines ruptured, so it had to be turned down to 20psi (after the 3rd data point) so the patched line would not break. Sampling was done periodically by removing the vessel, opening it, weighing the plates (in the same order each time), resealing the vessel, returning it to the incubator and noting the time it was returned, sparging at 250 mL/min, and turning the gas flow rate down to 40 mL/min. At the first sampling, the glass was observed to be cracking along the edges. Care was taken to make sure that the glass still adequately sealed off the vessel. Contamination was found in most of the plates at various time points. Contamination appeared as a slimy yellow substance, and was accompanied by a change in the color of the plate indicating a drop in medium pH. The appearance of contamination did not seem to affect the evaporation, so a note was made of which plates became contaminated and when the contamination appeared. The presence of contamination was accounted for in the data analysis.

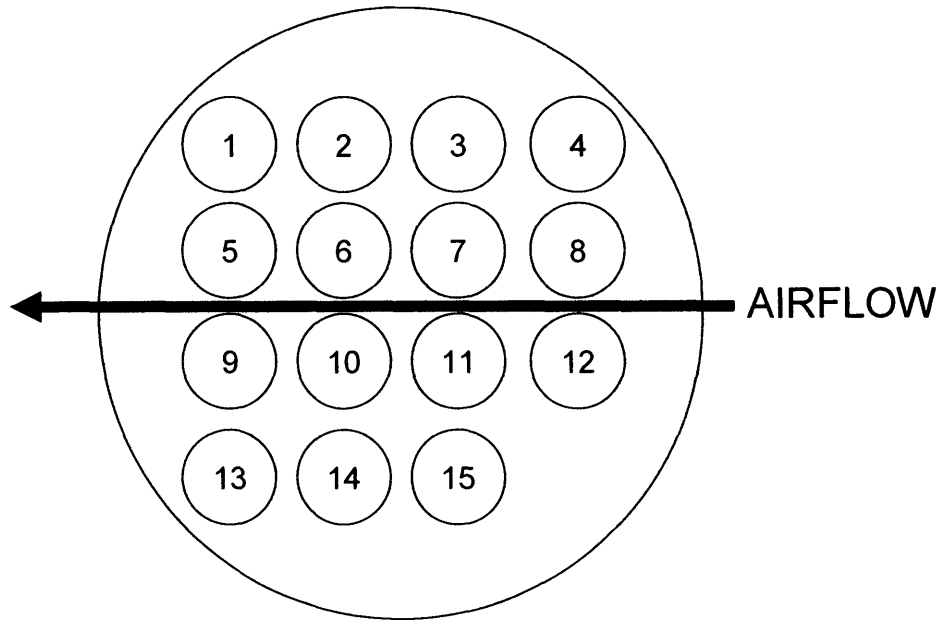

Figure 2-5: Plate arrangement for convective medium evaporation experiment. Fifteen 6 cm plates were placed without lids in the large reactor in the arrangement shown. Plates were returned to the same position after weighing to determine if evaporation was a function of position within the reactor.

3 Results

3.1 Medium Evaporation

	Evaporation Rate ± 95% Confidence Interval (mg/hr)
6-Well Plate	9.8 ± 0.4
½ of 6-Well Plate	12.9 ± 0.3
6 cm Plate (Convective)	11.0 ± 0.9
6 cm Plate	7.0 ± 0.2
10 cm Plate	10.6 ± 0.7

Table 3-1: Medium evaporation rate

The evaporation rate for 6-well plates, 6 cm plates, and 10 cm plates in a humidified 360 Series Steri-Cycle incubator; half-full 6-well plates in a humidified ThermoForma 360 Series Steri-Cycle incubator; and 4 cm plates in the reaction vessel are tabulated in Table 3-1. Individual evaporation rates were calculated for six 6-well plates, six 5 cm plates, six 10 cm plates, three half-full 6-well plates, and fifteen 6 cm plates (in the reaction vessel) via linear regression. The slopes were then averaged to calculate the mean values reported. Note that evaporation is 32% faster in a 6-well plate if only half the wells are being used, and that convective mass transfer increases the evaporation rate by 57%. Also note that the evaporation rates are not the same for a 6-well plate, a 6 cm plate, and a 10 cm plate. Evaporation occurs at nearly the same rate in 6-well plates and 10 cm plates, but a 6 cm plate's evaporation rate is only 71% of a 6-well plate's evaporation rate. A breakdown of these evaporation rates divided by the surface area can be seen in Table 3-2. The increase in mass transfer in 6 cm plates due to convection makes sense because the presence of convection tends to decrease the concentration of vapor near the gas-liquid interface and therefore increase the evaporation driving force. Similarly, the increase in evaporation rate with surface area makes sense due to the greater interfacial area over which evaporation can occur and greater gas volume above the liquid. Finally, the increase in evaporation rate when fewer wells are filled in a 6-well plate makes sense because the headspace vapor concentration will increase more slowly due to less vapor-liquid interfacial area, and therefore the concentration driving force will be greater. Evaporation results were used in later studies so that the metabolite concentrations could be adjusted to account for the concentration increases due to water lost to evaporation.

Plate	Surface Area (cm^2)	Evaporation Rate (mg/hr)	Rate/Area (mg/hr-cm^2)
6 cm	21	7.0	0.33
6-Well	57.6	9.8	0.17
10 cm	58.95	10.6	0.18

Table 3-2: Evaporation rates and surface areas for tissue culture plates

Since contamination appeared in most of the plates during the convective evaporation study, it is important to see if its presence affected the evaporation rate. Several plates had at least 2 uncontaminated data points, and at least 2 contaminated data points, which allowed evaporation rates to be calculated for both the uncontaminated portion and the contaminated portion of the experiment. A summary of the calculations for these plates can be seen in Table 3-3. Note that in six out of eight cases, evaporation occurred at a higher rate when something was growing in the plate than when the plate was sterile. A more comprehensive treatment of the contamination present in the study can be seen in Appendix C, where it is shown that the evaporation rate was slowest in the uncontaminated plate. These results are important because they suggest that cell-free evaporation rates are not the same as evaporation rates when cells are present.

Plate	Uncontaminated Evaporation (mg/h)	Contaminated Evaporation (mg/hr)
2	9.0	8.9
3	6.3	10.2
5	10.3	8.8
7	5.9	9.7
9	7.2	11.4
10	6.5	10.0
14	7.2	10.5
15	7.9	24.4

Table 3-3: Comparing contaminated evaporation rate with uncontaminated evaporation rate for the 6 cm convective evaporation study. Only plates for which slopes could be calculated for both the contaminated and uncontaminated regions are included in the table.

3.2 Metabolism and Kinetics: Incubator

A graphical depiction of cellular growth kinetics in an incubator can be seen in Figure 3-1, and of glucose-lactate metabolism in Figure 3-2. Data for the figures were taken during the incubator control experiment. In Figure 3-1, the numbers of viable cells are plotted as a function of time on a semi logarithmic plot with the goal of identifying the exponential growth

phase of the cell life cycle. During exponential cell growth, the natural logarithm of the cell concentration plotted as a function of time will appear as a straight line. A dotted box was drawn around the data points that are nearly linear. The region of exponential growth was used as a guide for planning sampling times for later experiments. When the seeding concentration was scaled up to a 6 cm plate by multiplying it by the ratio of the two areas, it was assumed that cells would exhibit growth behavior similar to the control experiment. Since the number of plates that fit in the large reaction vessel was limited, sampling times were planned so that they would be during the exponential growth phase of the control run to maximize the amount of useful data collected. The sampling times were then further refined after the first set of metabolism and kinetics experiments. Note that the doubling time was found to be 12.6 ± 0.6 hours, where the doubling time was calculated through linear regression, and the error was calculated via error propagation from the slope of the linear regression line.

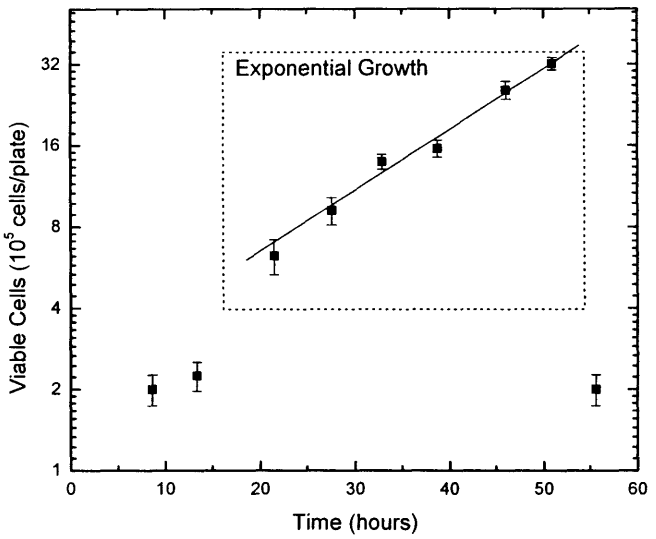

Figure 3-1: Stem cell growth over time under standard incubator growth conditions. The boxed area indicates the range of exponential growth over which the growth rate was calculated. Doubling time was found to be 12.6 ± 0.6 hours, where the error is equal to the standard error of the fit. Data points are the average of three samples taken at each time, and the error bars are equal to the standard deviation of the three samples.

The glucose and lactate concentrations from the control experiment were plotted to determine if there was a linear dependence, and to calculate the slope of the linear regression line (which is equal to the yield coefficient). In Figure 3-2, data points depicted are the mean metabolite concentrations at each time point. Error bars are equal to the standard deviations of the means. The yield of glucose to lactate was reported as g/g instead of mol/mol (as it was for the other yields) because one molecule of glucose is converted to two molecules of lactate, and glucose has twice the molecular weight of lactate. Therefore, at full conversion, there is 100% conversion of glucose to lactate on a g/g basis. Note that the points in the graph are nearly linear, and that there is 113% conversion of glucose to lactate. Also note that even two standard errors lower than the reported yield is a yield 3% higher than 100% conversion. This observation and the question of how this could be possible led to the development of the plating efficiency and metabolism and kinetics experiments to determine if oxygen is needed for stem cell culture, since a 100% conversion would suggest that metabolism may be entirely anaerobic.

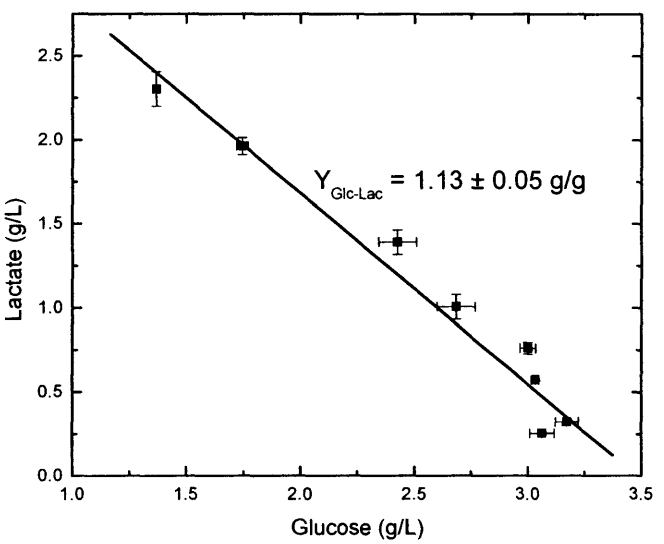

Figure 3-2: Glucose/lactate metabolism under standard incubator cell culture conditions. Each data point represents the average glucose and lactate concentrations at each time point. Error bars are equal to the standard deviation at each time point. Means and standard deviations come from measurements done in triplicate. The line is the best-fit line obtained through linear regression.

3.3 Plating Efficiency

A summary of the plating efficiency as a function of headspace oxygen concentration can be seen in Figure 3-3. The plating efficiency experiments were done to determine if the results of previously published studies (Wiles, 1993; Potocnik, 1994; Gassmann, 1996), in which plating efficiency was seen to increase as the oxygen concentration decreased, were reproducible. The plating efficiencies for two sets of experiments are plotted as a function of oxygen concentration.

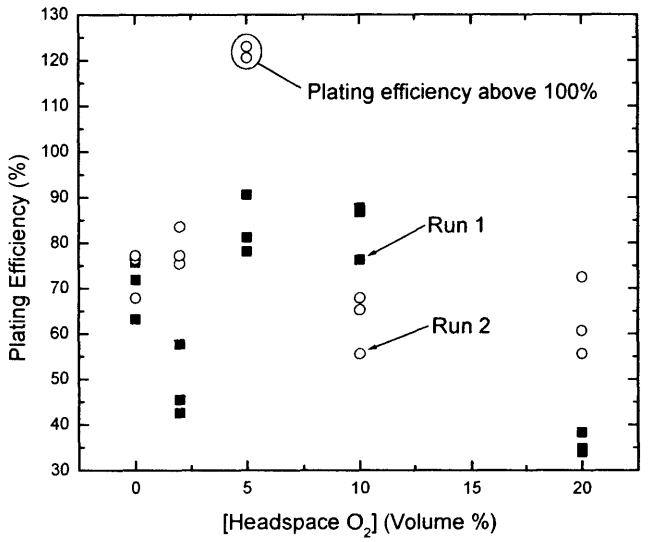

Figure 3-3: Plating efficiency as a function of headspace oxygen concentration. The plating efficiency experiment was done twice to see if the trends were reproducible. The first run is depicted as closed squares, and the second run as open circles. Probability that plating efficiency and oxygen concentration are correlated (based on data points from both runs) is 48%.

Note that there is no definitive evidence that plating efficiency and oxygen concentration are correlated, as there is only a 46.9% probability of correlation. Each data point is a plating efficiency calculated from the colonies counted on one plate. Also note that two plates gave plating efficiencies above 100%, which is impossible given the definition of plating efficiency. The results from this study were inconclusive. While more experimentation may have led to establishing a trend in the data, promising trends became apparent in the metabolism and kinetics experiments, so the focus of the experiment was shifted more heavily in favor of exploring the trends in the metabolism and kinetics studies.

3.4 Metabolism and Kinetics: Reaction Vessel

To determine the effect that changing the oxygen concentration has on stem cell growth and metabolism, two sets of experiments were done in the large reaction vessel whereby cell and metabolite concentrations were measured as a function of time and oxygen concentration. Because the vinyl lid used in the first experiment stretched and started to sag into the plates, a hard Lexan® plastic lid was used for the second run. A depiction of this sagging behavior can be seen in Figure 3-4. The sagging likely disrupted the air flow in the vessel, especially towards in the later runs, so the lid was changed in the second set of experiments. Since some of the data points in the first metabolism and kinetics experiment were outside the exponential growth phase of the cell lifecycle, the sampling interval for the second experiment were more closely spaced together so that all data points would be in the exponential growth phase. Otherwise the protocol followed for the two metabolism experiments was identical (2.6.4 and 2.6.5). All of the following graphs and tables in section 3.4 are from these two experiments.

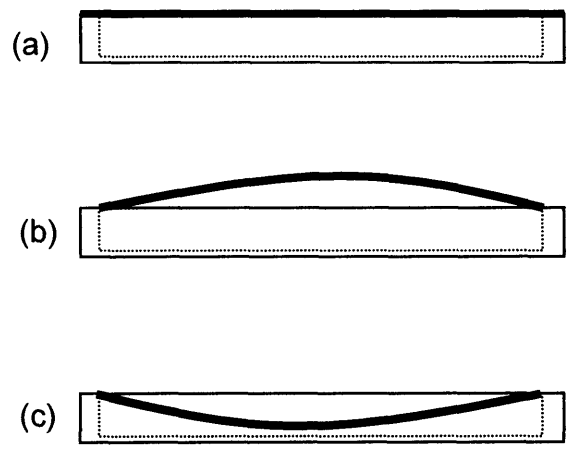

Figure 3-4: Behavior of the vinyl lid. The original placement of the vinyl lid can be seen in (a). When the gas was sparged through the reaction vessel to flush it, the vinyl stretched due to the increased pressure (b). After the flow through the reactor was reduced, the vinyl lid was no longer tight across the reactor and sagged onto the plates (c). Because this sagging likely caused gas flow disturbances, a hard Lexan® lid was used for the second set of experiments.

3.4.1 Oxygen Concentrations

Unfortunately, it was not possible to get as airtight a seal with Lexan® as it had been with vinyl, so oxygen concentrations were higher in the second run, as can be seen in Table 3-4.

Target [Headspace O_2]	Run 1 O_2 Range (vinyl)		Run 2 O_2 Range (Lexan®)	
	Minimum	Maximum	Minimum	Maximum
0%	0.0%	0.2%	0.4%	1.5%
2%	2.0%	2.5%	2.6%	3.2%
5%	6.2%	6.4%	6.8%	8.2%
10%	9.6%	11.2%	10.9%	14.3%
21%	20.9%	20.9%	20.9%	20.9%

Table 3-4: Range of headspace oxygen concentrations measured during each run. Values are given in percent oxygen saturation.

3.4.2 Growth Kinetics

The cell concentrations as a function of time and oxygen concentration are given in Figure 3-5. This plot serves to identify the regions over which cell growth was exponential (linear on the semi logarithmic plot) for the first metabolism and kinetics run.

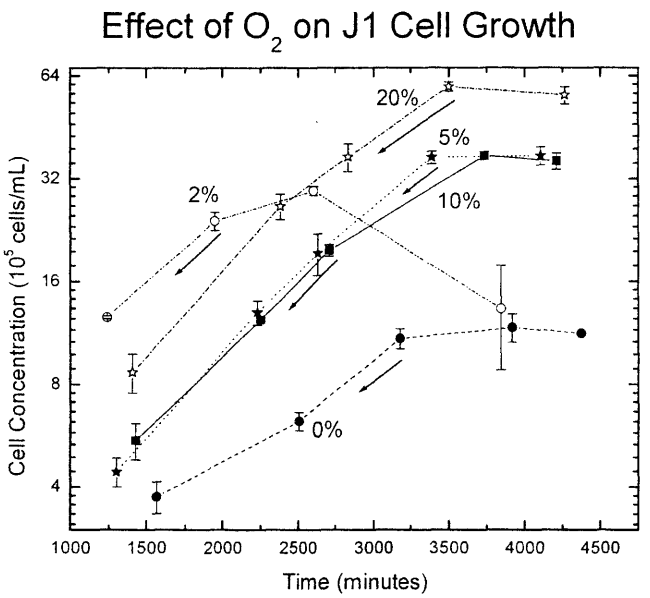

Figure 3-5: Cell growth in the reaction vessel: run 1

Data points depicted are the mean cell concentration at each time point. Error bars are equal to the standard deviation of the mean. The range from the first data point to the point with the backward facing arrow was used for calculating growth kinetics. The cutoff point was selected such that the slope between the cutoff point and the next point was visibly lower than the slope of the line passing through the points leading up to the cutoff point.

The range over which the cell growth was exponential in the first run was used to choose sampling times for the second run. The data points for the second run were spaced such that they all were in the exponential growth region (Figure 3-6). Note that all data points in the second set of experiments exhibited exponential growth, in that five sets of approximately linear data are visible.

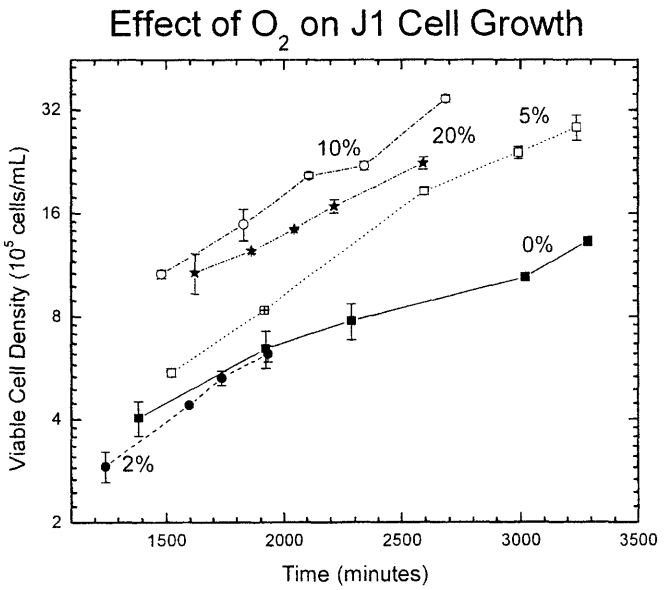

Figure 3-6: Cell growth in the reaction vessel: run 2

Doubling times were calculated from the data presented in Figure 3-5 and Figure 3-6 by fitting a line through the natural logarithm of the cell densities, and are reported in Table 3-5. The error reported was calculated via error propagation from the standard error of the linear regression slope. (See Appendix A.5 for the equations used.) Note that cell growth is slowest at the extreme concentration values, when doubling time is the longest. Compared to the incubator control doubling time of 12.6 $\pm$ 0.6 hours, there is a 17% chance that the first run doubling time at 20% oxygen is statistically different, and a 91% chance that the second run doubling time is statistically different.

[O2]	Doubling Time (h)	
	Run 1	Run 2
0%	18 ± 1	20 ± 1
2%	12.7 ± 0.7	10.2 ± 0.6
5%	11.3 ± 0.5	11.9 ± 0.5
10%	11.5 ± 0.5	12.2 ± 0.7
20%	12.5 ± 0.7	14.9 ± 0.9

Table 3-5: Doubling time as a function of headspace oxygen concentration

A probability table for doubling times from the two metabolism and kinetics runs is given in Table 3-6. Values reported are the probability that differences in doubling times for each run are statistically significant. Comparisons are within a run; no figures are reported for the differences between the first and second run. Since the two runs had different gas concentrations (Table 3-4), and because the second set of data did not include the stationary and death phase of the cell lifecycle, no statistical tests were done to compare the first set of data to the second.

	Run 1					Run 2				
	0%	2%	5%	10%	20%	0%	2%	5%	10%	20%
0%	X	97.4	100.0	100.0	99.8	X	100.0	100.0	100.0	98.2
2%	97.4	X	64.0	72.2	9.2	100.0	X	90.1	94.5	100.0
5%	100.0	64.0	X	18.9	82.9	100.0	90.1	X	34.2	99.5
10%	100.0	72.2	18.9	X	63.5	100.0	94.5	34.2	X	97.8
20%	99.8	9.2	82.9	63.5	X	98.2	100.0	99.5	97.8	X

Table 3-6: Probability (in percent) that doubling times are statistically different. The value 'X' is given where the statistical test of comparing a number to itself would be meaningless.

Note that many of the percentages are above 95%, indicating that the appropriate pair of doubling times is statistically different. Also note that most of the differences between the 20% doubling time and the other doubling times are more likely due to real differences than to random chance.

3.4.3 Maximum Cell Concentration

A summary of the maximum cell concentration reached in the first metabolism and kinetics run is given in Table 3-7. Only the first run is tabulated because the second run was only run over the exponential growth phase of the cell life cycle, so the cells never reached their

maximum sustainable cell concentration. The peak cell concentrations from the data presented in Figure 3-5 are reported.

[O2]	Maximum Cell Density (10^6 cells/plate)
0%	2.50
2%	6.08
5%	8.00
10%	7.66
20%	12.29

Table 3-7: Maximum cell densities reached at various oxygen concentrations. Probability of correlation = 97%.

Note here that there is a very high probability (97%) that maximum cell concentration is correlated with the headspace oxygen concentration.

3.4.4 Plating Efficiency

Plating efficiencies were calculated from the metabolism and kinetics runs by extrapolating the exponential growth curves (Figure 3-5 and Figure 3-6) backwards to time zero. The number initial number of cells predicted by the growth curve was divided by the number of cells plated to yield the plating efficiency. The results of these calculations can be seen below in Table 3-8.

	Plating Efficiency (%)	
DO (%)	Run 1	Run 2
0%	49.6	50.2†
2%	99.9†	17.7†
5%	63.0†	31.6
10%	33.8	63.7†
20%	62.5†	71.0
	Correlation Probability	
Condition	Run 1	Run 2
$[O_2]$	29.4	84.4
Passaged?	85.9	24.3

Table 3-8: Plating efficiency from metabolism and kinetics runs, and the probability they are correlated with headspace oxygen or whether or not they had been passaged. The probability that the plating efficiency and oxygen concentration are correlated is given in the first row of the correlation table. The probability that plating efficiency is correlated with whether of not the cells were passaged is given in the second row.
†: Cells were passed at least once after thawing and before seeding.

Probability of correlation with whether or not cells had been passed between thawing and seeding was calculated by setting x equal to 1 if they had been passed, and 0 if they had not been passed. Values of y were the associated plating efficiencies. Note that in the first run, the data were more correlated with whether cells had been passed or not than with headspace oxygen concentration. Also note that the trend is the opposite in the second run, indicating once again that plating efficiency results were not reproducible.

3.4.5 Overall Metabolism

A graphical depiction of typical metabolite levels as function of time during the metabolism and kinetics experiments can be seen in Figure 3-7. The chart is given for the first run under 0% oxygen. Note that glucose and glutamine concentrations are clearly decreasing, and that lactate and ammonia concentrations are clearly increasing with time. Although glutamate concentration appears to be decreasing with time, the error bars are large relative to the amount of increase. These trends were seen throughout the metabolism kinetics runs, and can be seen in Table 3-9.

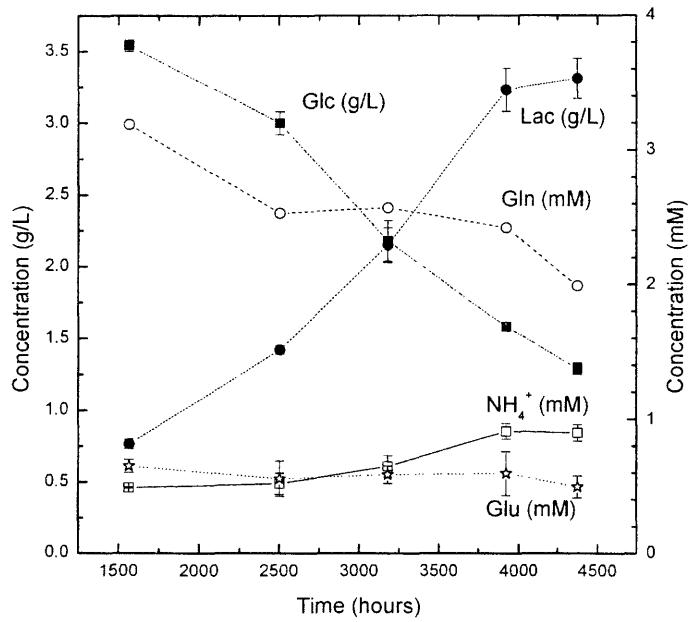

Figure 3-7: Metabolism under apoxic growth conditions

			Run 1					Run 2				
0%	Sample		1	2	3	4	5	6	7	8	9	10
	Time	(minutes)	1565	2505	3180	3920	4375	1385	1920	2285	3020	3285
	Glucose	(g/L)	3.54 ± 0.04	3 ± 0.08	2.18 ± 0.14	1.58 ± 0.01	1.29 ± 0.04	3.48 ± 0.02	3.17 ± 0.01	3.01 ± 0.03	2.17 ± 0.08	1.75 ± 0.05
	Lactate	(g/L)	0.77 ± 0.03	1.42 ± 0.03	2.15 ± 0.12	3.23 ± 0.15	3.31 ± 0.14	0.73 ± 0.05	1.07 ± 0.02	1.32 ± 0.05	2.16 ± 0.08	2.68 ± 0.07
	Glutamine	(mM)	3.2 ± 0.1	2.5 ± 0.7	2.6 ± 0.2	2.4 ± 0.5	2 ± 0.3	3.6 ± 0.5	2.2 ± 0.4	2.6 ± 0.7	1.8 ± 0.3	1.6 ± 0.2
	Glutamate	(mM)	0.65 ± 0.05	0.56 ± 0.13	0.59 ± 0.07	0.6 ± 0.16	0.5 ± 0.08	0.55 ± 0.11	0.31 ± 0.08	0.43 ± 0.16	0.32 ± 0.07	0.31 ± 0.02
	NH4+	(mM)	0.487 ± 0.006	0.52 ± 0.079	0.647 ± 0.08	0.913 ± 0.059	0.9 ± 0.061	0.313 ± 0.015	0.357 ± 0.006	0.327 ± 0.006	0.493 ± 0.012	0.573 ± 0.058
2%	Sample		1	2	3	4		6	7	8	9	
	Time	(minutes)	1240	1950	2605	3845		1245	1595	1735	1930	
	Glucose	(g/L)	2.93 ± 0.03	1.78 ± 0.02	1.13 ± 0.03	0.88 ± 0.04		3.66 ± 0.04	3.54 ± 0.07	3.52 ± 0.08	3.29 ± 0.03	
	Lactate	(g/L)	1.16 ± 0.02	2.33 ± 0.08	3.3 ± 0.2	3.56 ± 0.25		0.47 ± 0.01	0.64 ± 0.01	0.7 ± 0.01	0.77 ± 0.01	
	Glutamine	(mM)	2.3 ± 0.8	1.6 ± 0.6	1.4 ± 0.4	1.4 ± 0.1		1.9 ± 0.4	2 ± 0.5	1.8 ± 0.1	2.3 ± 0.1	
	Glutamate	(mM)	0.45 ± 0.17	0.38 ± 0.15	0.37 ± 0.11	0.42 ± 0.06		0.26 ± 0.08	0.33 ± 0.09	0.28 ± 0.01	0.41 ± 0.02	
	NH4+	(mM)	0.433 ± 0.121	0.75 ± 0.01	0.91 ± 0.01	1.103 ± 0.085		0.32 ± 0.026	0.337 ± 0.042	0.373 ± 0.031	0.4 ± 0.04	
5%	Sample		1	2	3	4	5	6	7	8	9	10
	Time	(minutes)	1305	2230	2635	3390	4105	1520	1915	2595	2990	3240
	Glucose	(g/L)	3.58 ± 0.04	2.97 ± 0.09	2.6 ± 0.15	1.36 ± 0.02	1.1 ± 0.02	3.5 ± 0.02	3.29 ± 0.01	2.73 ± 0.15	2.05 ± 0	1.79 ± 0.04
	Lactate	(g/L)	0.49 ± 0.01	1.13 ± 0.02	1.57 ± 0.07	2.64 ± 0.23	3.24 ± 0.13	0.54 ± 0	0.72 ± 0	1.4 ± 0.05	1.94 ± 0.05	2.46 ± 0.15
	Glutamine	(mM)	2 ± 0.2	1.8 ± 0.4	1.8 ± 0.3	1.3 ± 0.2	0.8 ± 0.1	2.2 ± 0.1	1.8 ± 0.3	1.3 ± 0.8	1.6 ± 0.3	1.7 ± 0.7
	Glutamate	(mM)	0.28 ± 0.04	0.33 ± 0.09	0.37 ± 0.08	0.36 ± 0.08	0.27 ± 0.03	0.37 ± 0.02	0.33 ± 0.07	0.28 ± 0.2	0.22 ± 0.02	0.34 ± 0.16
	NH4+	(mM)	0.27 ± 0.02	0.377 ± 0.029	0.42 ± 0.061	0.777 ± 0.015	0.94 ± 0.066	0.275 ± 0.021	0.28 ± 0	0.35 ± 0.085	0.5 ± 0	0.5 ± 0.042
10%	Sample		1	2	3	4	5	6	7	8	9	10
	Time	(minutes)	1430	2250	2710	3735	4210	1480	1830	2110	2340	2685
	Glucose	(g/L)	3.28 ± 0.09	2.77 ± 0.05	2.39 ± 0.12	1.11 ± 0.02	0.96 ± 0.03	3.75 ± 0.03	3.22 ± 0.1	2.68 ± 0.04	2.37 ± 0.04	1.86 ± 0.04
	Lactate	(g/L)	0.57 ± 0.03	1.14 ± 0.06	1.64 ± 0.03	2.79 ± 0.08	3.12 ± 0.17	0.81 ± 0	1.13 ± 0.03	1.3 ± 0.08	1.51 ± 0.04	2.02 ± 0.05
	Glutamine	(mM)	1.8 ± 0.2	1.5 ± 0	1.2 ± 0	0.7 ± 0	0.6 ± 0.1	1.6 ± 0.1	1.5 ± 0.1	1.4 ± 0.1	1.3 ± 0.1	1 ± 0
	Glutamate	(mM)	0.41 ± 0.06	0.38 ± 0.05	0.34 ± 0.01	0.36 ± 0.01	0.35 ± 0.01	0.22 ± 0.01	0.26 ± 0.03	0.27 ± 0.03	0.3 ± 0.02	0.27 ± 0.01
	NH4+	(mM)	0.263 ± 0.021	0.367 ± 0.047	0.493 ± 0.081	0.93 ± 0.075	1.063 ± 0.05	0.417 ± 0.009	0.39 ± 0.053	0.483 ± 0.083	0.49 ± 0.099	0.62 ± 0
20%	Sample		1	2	3	4	5	6	7	8	9	10
	Time	(minutes)	1410	2380	2835	3500	4265	1620	1860	2045	2215	2590
	Glucose	(g/L)	3.46 ± 0.09	2.68 ± 0.06	2.08 ± 0.06	1.36 ± 0.04	1.02 ± 0.01	3.36 ± 0.07	3.26 ± 0.05	3.15 ± 0.05	3.05 ± 0.06	2.78 ± 0.09
	Lactate	(g/L)	0.66 ± 0.03	1.61 ± 0.03	2.12 ± 0.16	2.68 ± 0.09	3.22 ± 0.15	0.69 ± 0.01	0.81 ± 0.03	0.95 ± 0.03	1.08 ± 0.05	1.48 ± 0.04
	Glutamine	(mM)	2.5 ± 0.3	1.6 ± 0.3	1.2 ± 0.5	0.5 ± 0.1	0.2 ± 0.1	2 ± 0.1	2.2 ± 0.4	1.9 ± 0.2	1.8 ± 0.3	1.8 ± 0.4
	Glutamate	(mM)	0.46 ± 0.05	0.4 ± 0.06	0.37 ± 0.12	0.37 ± 0.12	0.37 ± 0.07	0.28 ± 0.04	0.41 ± 0.04	0.4 ± 0.06	0.34 ± 0.11	0.45 ± 0.14
	NH4+	(mM)	0.52 ± 0.04	0.543 ± 0.068	0.67 ± 0.026	0.993 ± 0.057	1.22 ± 0.092	0.357 ± 0.038	0.46 ± 0.03	0.477 ± 0.038	0.537 ± 0.006	0.563 ± 0.038

Table 3-9: Metabolite profiles as a function of time and oxygen concentration. Values reported are the mean ± 1 standard deviation for each data point. Standard deviation is reported as zero when only one data point is available, or when all data points were measured to be the same value.. The first 2% experiment was terminated early due to low viability. The second 2% experiment was terminated early because the source gas tank was nearly empty.

3.4.6 $Y_{Lac/Glc}$

Glucose-lactate calculations for the two metabolism and kinetics runs were done in three different ways. The first way is the method traditionally used in cell culture where glucose and lactate concentrations are measured and used directly. The second set of calculations were done to account for the amount of evaporation that occurred and the corresponding effect on the measured metabolite concentrations. The third set of calculations accounted for both evaporation and the effects that pyruvate in stem cell medium has on the carbon balance.

3.4.6.1 Uncorrected Glucose-Lactate Yields

Uncorrected glucose-lactate yields from the metabolism and kinetics experiments are given in Table 3-10, where the reported values are percentage of glucose mass converted to lactate mass. Error given is the standard error of the regression line. Note that yield and oxygen concentration appear to be negatively correlated in the first run, and that no correlation is obvious for the second run. Also note that most of the yields are above 100%, which does not make sense from a materials balance standpoint.

	$Y_{Lac/Glc}$ (% g/g)	
[O2]	**Run 1**	**Run 2**
0%	117 ± 5	111 ± 2
2%	118 ± 7	60 ± 10
5%	105 ± 4	107 ± 6
10%	105 ± 4	59 ± 4
20%	99 ± 4	130 ± 10

Table 3-10 Uncorrected glucose to lactate yield (g/g)

Probabilities that differences between yields within a metabolism and kinetics run are statistically significant are given in Table 3-11. Note that, in all cases, hypoxia results in a glucose-lactate yield that is different from the yield at atmospheric conditions, and that the probability is greater than 50% that these differences are statistically significant

	Run 1					Run 2				
	0%	2%	5%	10%	20%	0%	2%	5%	10%	20%
0%	X	13.6	91.4	92.8	98.9	X	100.0	55.9	100.0	87.4
2%	13.6	X	89.0	90.6	97.9	100.0	X	93.7	17.5	99.4
5%	91.4	89.0	X	3.9	63.0	55.9	93.7	X	100.0	79.4
10%	92.8	90.6	3.9	X	69.4	100.0	17.5	100.0	X	100.0
20%	98.9	97.9	63.0	69.4	X	87.4	99.4	79.4	100.0	X

Table 3-11: Probability (in percent) that glucose-lactate yields are statistically different. The value 'X' is given where the statistical test of comparing a number to itself would be meaningless.

3.4.6.2 Corrected Glucose-Lactate Yields

Glucose-lactate yields corrected for evaporation, and yields corrected for both evaporation and pyruvate are given in Table 3-12, where the reported values are percentage of glucose mass converted to lactate mass. Data were taken during the metabolism and kinetics runs. Error reported is the standard error of the regression line. Note that correcting for evaporation brings all of the yields below the theoretical limit of 100%. Also note that the same trends are evident (yield decreases with increasing oxygen concentration for the first run, and has no obvious correlation with oxygen concentration for the second run), even though the yields are lower than previously reported.

	With Evaporation		With Evaporation and Pyruvate	
	$Y_{Lac/Glc}$ (% g/g)		$Y_{Lac/Glc}$ (% g/g)	
	Run 1	Run 2	Run 1	Run 2
0%	89 ± 4	88 ± 1	88 ± 4	86 ± 1
2%	94 ± 6	50 ± 9	92 ± 6	49 ± 8
5%	84 ± 3	87 ± 5	83 ± 3	86 ± 5
10%	84 ± 3	50 ± 4	82 ± 3	50 ± 4
20%	77 ± 3	95 ± 8	75 ± 3	95 ± 8

Table 3-12: Corrected Glucose-Lactate Yield (g/g)

The correlation between the glucose-lactate yields and oxygen concentration is expressed mathematically in Table 3-13. Note that there is a high probability of correlation for the first run, and a lower probability of correlation for the second run. Also note that correcting the measured yields for evaporation and pyruvate does not have a major effect on the strength of the correlation.

	Probability of Correlation (%)	
	Run 1	Run 2
Uncorrected	95.3	42.8
Evaporation Corrected	95.4	34.5
Evaporation and Pyruvate Corrected	97.2	35.8

Table 3-13: Probability that yields are correlated with $[O_2]$

Probabilities that pairs of evaporation-corrected yields within a run are statistically different are given in Table 3-14, and probabilities for evaporation and pyruvate-corrected yields are given in Table 3-15. Note that the same trends that were apparent with the uncorrected yields are apparent here. (Hypoxia results in a glucose-lactate yield that is different from the yield at atmospheric conditions, and that the probability is greater than 50% that these differences are statistically significant.) The only exception is that the difference between the 5% and 20% yields in the second metabolism and kinetics runs is now less than 50% likely to be statistically significant.

	Run 1					Run 2				
	0%	**2%**	**5%**	**10%**	**20%**	**0%**	**2%**	**5%**	**10%**	**20%**
0%	X	45.9	66.9	72.2	97.2	X	100.0	5.4	100.0	70.3
2%	45.9	X	83.9	86.8	98.0	100.0	X	97.9	0.1	99.8
5%	66.9	83.9	X	6.4	86.0	5.4	97.9	X	100.0	45.6
10%	72.2	86.8	6.4	X	86.5	100.0	0.1	100.0	X	100.0
20%	97.2	98.0	86.0	86.5	X	70.3	99.8	45.6	100.0	X

Table 3-14: Probability (in percent) that evaporation-corrected yields are statistically different. The value 'X' is given where the statistical test of comparing a number to itself would be meaningless.

	Run 1					Run 2				
	0%	**2%**	**5%**	**10%**	**20%**	**0%**	**2%**	**5%**	**10%**	**20%**
0%	X	44.9	67.1	76.4	98.0	X	100.0	17.6	100.0	74.7
2%	44.9	X	83.5	88.0	98.4	100.0	X	98.1	0.9	99.8
5%	67.1	83.5	X	17.0	90.0	17.6	98.1	X	100.0	45.7
10%	76.4	88.0	17.0	X	86.8	100.0	0.9	100.0	X	100.0
20%	98.0	98.4	90.0	86.8	X	74.7	99.8	45.7	100.0	X

Table 3-15: Probability (in percent) that evaporation and pyruvate-corrected yields are statistically different. The value 'X' is given where the statistical test of comparing a number to itself would be meaningless.

3.4.7 $Y_{NHx/Gln}$

Yield of glutamine to ammonia in the metabolism and kinetics experiments is given in Table 3-16. Yields reported are molar yields, and are corrected for evaporation. The probabilities that pairs of yields within each run are statistically significant are given in Table 3-17. Note that the data are inconclusive, as no trend is readily apparent.

	$Y_{NHx/Gln}$ (% mM/mM)	
[O2]	Run 1	Run 2
0%	11 ± 5	6 ± 2
2%	23 ± 6	-2 ± 5
5%	34 ± 4	3 ± 7
10%	37 ± 4	25 ± 8
20%	19 ± 4	10 ± 6

Table 3-16: Conversion of glutamine to ammonia (mM/mM)

	Run 1					Run 2				
	0%	2%	5%	10%	20%	0%	2%	5%	10%	20%
0%	X	87.0	99.7	99.9	75.8	X	89.0	48.6	95.9	38.1
2%	87.0	X	86.2	93.6	44.0	89.0	X	42.2	99.0	84.6
5%	99.7	86.2	X	35.8	97.3	48.6	42.2	X	88.4	51.6
10%	99.9	93.6	35.8	X	99.0	95.9	99.0	88.4	X	81.9
20%	75.8	44.0	97.3	99.0	X	38.1	84.6	51.6	81.9	X

Table 3-17: Probability (in percent) that differences between ammonia-glutamine yields are statistically significant The value 'X' is given where the statistical test of comparing a number to itself would be meaningless.

3.4.8 $Y_{VC/Glu}$

The yield of glucose to viable cells in the metabolism and kinetics experiments is tabulated in Table 3-18. Values were calculated for data points up to the peak concentration for the first run, and from all data points for the second run. Note that magnitude of the yield increases with increasing oxygen concentration. Table 3-19 gives the probabilities that pairs of yields within each run are statistically different. Note here that most of the apparent differences in yield are statistically significant, in that the probability is greater than 95%.

[O2]	$Y_{VC/Glc}$ (10^6cells/mmol)	
	Run 1	Run 2
	0.040 ± 0.003	0.046 ± 0.003
2%	0.091 ± 0.004	0.061 ± 0.009
5%	0.140 ± 0.005	0.117 ± 0.006
10%	0.13 ± 0.02	0.12 ± 0.01
20%	0.22 ± 0.01	0.166 ± 0.009

Table 3-18: Yield of glucose to viable cells (10^6 cells/mmol)

	Run 1					Run 2				
	0%	2%	5%	10%	20%	0%	2%	5%	10%	20%
0%	X	100.0	100.0	100.0	100.0	X	82.7	100.0	100.0	100.0
2%	100.0	X	100.0	96.0	100.0	82.7	X	99.4	90.4	100.0
5%	100.0	100.0	X	32.5	100.0	100.0	99.4	X	4.4	99.8
10%	100.0	96.0	32.5	X	100.0	100.0	90.4	4.4	X	96.8
20%	100.0	100.0	100.0	100.0	X	100.0	100.0	99.8	96.8	X

Table 3-19: Probability (in percent) that differences in glucose-cell yield are statistically significant. The value 'X' is given where the statistical test of comparing a number to itself would be meaningless.

In Table 3-20, the probabilities of correlation between headspace oxygen concentration and the reported glucose to viable cell yields are given for each run. Note that there is a very high probability that glucose-cell yield is correlated with oxygen concentration.

Run	Correlation Probability (%)
1	98.3
2	97.9

Table 3-20: Probability that glucose-cell yield is correlated with headspace oxygen concentration

3.4.9 $Y_{VC/Gln}$

The yield of glutamine to viable cells in the metabolism and kinetics experiments is tabulated in Table 3-21. Note that a trend isn't apparent in these data. Table 3-23 gives the probabilities that pairs of yields within each run are statistically different.

[O2]	$Y_{VC/Gln}$ (10^6 cells/mmol)	
	Run 1	Run 2
0%	0.2 ± 0.1	0.17 ± 0.04
2%	0.3 ± 0.2	-0.6 ± 0.60
5%	1.3 ± 0.3	0.5 ± 0.3
10%	1.0 ± 0.3	1.7 ± 0.2
20%	1.2 ± 0.2	0.4 ± 0.2

Table 3-21: Yield of glutamine to viable cells (10^6 cells/mmol)

Run	Correlation Probability (%)
1	81.7
2	73.2‡

Table 3-22: Probability that glutamine-cell yield is correlated with headspace oxygen concentration.
‡Probability for the second run doesn't include the data point at 2% oxygen because a negative yield doesn't make sense, as it implies that glutamine is produced with cell growth. See 3.4.9 for a more in-depth treatment of this issue.

	Run 1					Run 2				
	0%	2%	5%	10%	20%	0%	2%	5%	10%	20%
0%	X	87.0	99.7	99.9	75.8	X	97.2	79.8	100.0	81.1
2%	87.0	X	86.2	93.6	44.0	97.2	X	83.4	100.0	95.4
5%	99.7	86.2	X	35.8	97.3	79.8	83.4	X	99.4	11.4
10%	99.9	93.6	35.8	X	99.0	100.0	100.0	99.4	X	100.0
20%	75.8	44.0	97.3	99.0	X	81.1	95.4	11.4	100.0	X

Table 3-23: Probability (in percent) that differences in glutamine-cell yields are statistically significant. The value 'X' is given where the statistical test of comparing a number to itself would be meaningless.

4 Discussion

Three different lids were used during the metabolism and kinetics studies. A glass lid was originally used, but sealing the chamber during the medium evaporation study chipped the edges of the glass disc. A clear vinyl was used for the first metabolism and kinetics run as a replacement for the glass. However, the pressure of flushing the vessel caused the vinyl to stretch and begin to sag. A hard Lexan cover was used for the second run. The biggest effect that changing the lid had was how well the reactor sealed. In Table 3-4, it can be seen that there was less leaking occurring in the first run, as the gas concentrations are closer to that of the premixed cylinder. While the leaking problem wasn't severe enough to cause the five ranges to overlap, it is important to note that the parameters calculated in this study weren't based on a completely static headspace gas composition. As a result, error bars are indicative of both uncertainty in measurement and variation in headspace oxygen concentration. It's also important to note that the parameters from the second run are for up to 1% higher oxygen concentrations, so it may not be applicable to compare results from the first run to the second. For the most part, however, the trends observed in the first run were duplicated in the second run. From looking at the data, it appears that a stronger trend with more significant differences between data points can be seen in the kinetics data from the second run, and the metabolism data exhibit stronger correlations and greater data point resolution in the first run. This greater resolution of data points makes sense because the cells were allowed to grow for a longer time—as much as twice as long—during the first metabolism and kinetics run, and had more time to deplete the nutrients in the medium. Unfortunately, growing the cells for a longer time meant that data points were more spaced out, and kinetics calculations had to be done with as few as two data points. Calculating slopes with fewer data points led to greater error in the calculated value. In the second run, all five samples were taken during the exponential growth phase. While this meant that it was much easier to make accurate kinetics calculations, the cells were not always given ample time to cause significant changes in the medium composition. As the change in medium concentration shrinks, it can approach the error of the instrument, and prevent accurate yield calculations. The best example of this effect can be seen by looking at the growth data for the second run of 2% oxygen (Table 3-9),

where yield calculations are done based on concentrations that change very little over the course of the run. Error in the YSI biochemistry analyzer is 5%, and the glucose concentration changed by only 11% from the start to the finish of the experiment. As the magnitude of the error in the instrument is close to the magnitude of the measured concentration change, calculations based on the change in concentration values (as are yield calculations) are suspect. As the concentration changes become larger (as in the first metabolism and kinetics run), yield calculations can be expected to be more accurate.

4.1 Effect of evaporation

One of the most striking results of the metabolism and kinetics experiments was the effect that correcting for evaporation had on the yield calculations. Evaporation has been mentioned as a factor that can increase medium osmolarity over long-term cell growth. Having a humidified incubator is normally thought to solve the evaporation problem, but the average humidity of an incubator tends to be less than 100%, and it can take around an hour for an incubator's humidity to equilibrate after the door is opened for only 30 seconds (Potter & DeMarse, 2001). While Potter has discussed evaporation in the context of osmolarity, no one has mentioned the effect that medium evaporation has on metabolism calculations. An excellent example of how neglecting to account for medium evaporation can impact experimental conclusions can be seen by comparing Table 3-10 and Table 3-12. Without correcting for evaporation, we see conversion rates that are as much as 18% higher than 100%. Error bars given are the standard error of the calculated yield. Considering that the 95% confidence interval is approximately equal to twice the standard error, the conclusion can be drawn that the 0% and 2% yields from the first metabolism and kinetics run are statistically different from 100%. While there are other possible sources of lactate production in the cell than from glucose metabolism (i.e. from pyruvate that was added to the medium, or even from glutamine metabolism(Zielke et. al., 1980)), there are other ways for glucose to be consumed. Glucose is also used to fuel anabolic reactions and can be converted into alanine. Presented with yields greater than 100%, one paper has suggested that the pyruvate present in DMEM could be the source of the additional lactate (Gstraunthaler et. al., 1999). However, HPLC analysis in this study has shown that metabolism of the pyruvate present in medium is not always enough to account for yields above 100%. Pyruvate metabolism does affect yield calculations by a few percent, but not

nearly as much as evaporation of medium, which can affect the yield by more than 20%. It was surprising that no mention of correcting for evaporation was seen in the literature, especially considering the profound effect evaporation can have on the calculations. It is highly recommended that future experiments in cellular metabolism account for this crucial factor.

The trends apparent in Table 3-1 suggest a few interesting conclusions. One conclusion is that using 2 half-full six-well plates is not equivalent to using one full six-well plate from a metabolic standpoint, as evaporation is 32% faster when only 3 wells are used. Evaporation is probably faster in the half-full plate because fewer wells are supplying the vapor necessary to come to equilibrium. A second conclusion is that medium evaporates 57% faster in the reaction vessel than in a covered dish inside the incubator. This was expected, as gas flow is occurring over the surface of the medium as the reaction vessel is continually flushed, and is adding a convective driving force to the diffusive driving force. Yet another trend is apparent in the evaporation rates as a function of surface area. In terms of surface area, a 6 cm plate has 64% less area than a 6-well plate, which in turn has 2% less growth area than a 10 cm plate. Looking at Table 3-1, it is apparent that evaporation rate increases as surface area increases. However, it is not a linear dependence, as a 2% increase in area from a 6-well to a 10 cm plate results in an 8% increase in evaporation rate. This non-linearity could be due to differences in plate geometry.

Another factor that has to be taken into consideration in evaporation calculations is the effect that cell growth has on evaporation rate. While contamination was not expected, its appearance in the convective evaporation study makes sense because the vessel was opened in a non-sterile environment to weigh the plates. Initially, this was seen as an unfortunate occurrence, but some interesting trends became apparent when the data were analyzed. First of all, the plate in which no contamination was observed had an evaporation rate that was slower than the other 14 plates. Contamination was noted qualitatively by a change in the color of the medium from red to yellow, and by the appearance of a yellow residue. No attempt was made to quantify the degree of contamination. Furthermore, when evaporation rate could be broken down into contaminated and non-contaminated rates, the contaminated

rate was between 47% and 210% higher than the uncontaminated rate in 6 out 8 plates. These trends suggest that measuring the cell-free evaporation rate may not give the correct evaporation rate to be used when correcting metabolite concentrations. Evaporation probably occurs at a higher rate when cells (or bacteria) are actively growing in the plate because some of the metabolic products are either evaporating (like ammonia) or are released as gases (particularly carbon dioxide in the case of animal cells) that can diffuse into the headspace gases. While evaporation rates are likely to be different for animal cells than bacterial cells due to differences in cellular metabolism, both rates are likely to be higher than in cell-free systems. For the purposes of evaporation corrections in this study, the average rate (including the contaminated plates) was used. For more rigorous evaporation correction in the future, it would be better to determine evaporation rate as a function of plate size and viable cell concentration.

4.2 Growth rates and maximum cell density

An interesting trend can be seen in the two sets of doubling times tabulated in Table 3-5. In both instances, doubling time decreased as the headspace oxygen concentration dropped below atmospheric levels, and then increased again as the oxygen level approached zero. In the first run, there is a greater than 60% chance that cells grow faster at 5% to 10% oxygen than at 20% oxygen. While this is by no means statistical proof, it is evidence to suggest that there may be a trend. When all data points were taken during the exponential growth phase of the cell cycle, the evidence is much more conclusive, as the probabilities that cells grow faster at 2%, 5%, or 10% DO than at 20% DO are all greater than 97%. As the probabilities are greater than 95%, this evidence can be considered proof that stem cell growth occurs at a faster rate than at atmospheric oxygen levels. While cell growth was slowest in both runs when dissolved oxygen approaches zero, it could be that the cells were shocked from going directly from an incubator at 21% oxygen to a reaction vessel at 0% oxygen, and did not have adequate time to adapt to their new environment. Others have also come to the conclusion that ESC grow slower when DO drops below 2%. (Iyer et. al., 1998; Carmeliet et. al., 1998). Work with hybridoma cells has shown that cells do not grow when they are suddenly exposed to apoxic conditions, but they can adapt to growing in apoxic conditions if the process is a gradual adaptation instead of a sudden one. (Ozturk & Pallson, 1990). With a gradual

adaptation, it may be possible to get stem cells to grow faster in apoxic conditions than they grew in this study.

The most likely cause for increased rate of cellular proliferation at moderately hypoxic conditions is the resulting lower concentration of DNA-damaging free radicals. This makes sense from an embryological perspective, as the hypoxic environment of early development is known to protect the embryo before it has ways to deal with ROS. (Caniggia et. al., 2000; Orsi & Leese, 2001). Furthermore, the presence of a hypoxic environment is important because oxygen gradients in a developing embryo activate certain genes. (Adelman et. al., 2000).

While the first run did not provide as many data points in the exponential growth regime, it did provide data that the second run was unable to provide: the maximum sustainable cell density. These numbers are based on the highest cell density measured, but the data points were so widely spaced that it is impossible to know the exact peak of the curve. However, there are enough data points to see an obvious trend: decreasing headspace oxygen decreases the maximum sustainable cell concentration. The correlation is a very strong one, with a probability above 97%. This conclusion makes sense from a biological standpoint. Assuming that oxygen is a limiting factor in cell growth, the oxygen supply can only penetrate through a certain depth of cells before it is used up. Less oxygen implies a thinner layer of cells at steady state and therefore a lower cell concentration.

4.3 Carbohydrate metabolism

A few important trends can be seen by examining Table 3-12. In the first run, where more extensive metabolism was allowed to occur, there is an obvious trend to the data where decreasing the headspace oxygen concentration resulted in greater conversion of glucose to lactate. The probability of correlation, which is about 95%, supports the notion that glucose-to-lactate yield is correlated with the headspace oxygen concentration. However, there is no trend apparent in the experimental repeat. In particular, the data points for 2% and 10% oxygen do not make sense compared to the other 8 data points of the set. The deviation for the 2% point was likely caused by the relatively low amount of metabolism that occurred during the run (Table 3-9). The entire run had to be done over a short stretch of time because

the feed gas tank was running out. Although the measurements are fairly precise, the YSI instrument used to take the measurements is only accurate to ±5%. Considering this 5% interval around the initial and final glucose measurements of 3.66, 3.29, we get a range of 3.48 to 3.84 for the initial concentration, and a range of 3.13 to 3.45 for the final concentration. Looking at these ranges, it is apparent that the initial concentration isn't all that different from the final concentration, and the deviation of the calculated yield can be understood. The deviation of the second 10% data point could also be due to error in the instrumentation. Glucose and lactate measurements during this second 10% metabolism and kinetics run were consistently too high, and the instrument failed the linearity check. Since the results are suspect to begin with due to problems with the instrumentation, the deviation of the calculated yield from the expected behavior is understandable. Since the first run allowed a greater degree of metabolism to occur, it more likely estimates the true behavior of the cells, and it is the one from which conclusions should be drawn. The evaporation and pyruvate corrected yield at 20% oxygen was measured to be 77%, which would be equivalent to 1.54 mol/mol, since 1 mol of glucose can be completely converted to 2 mol of lactate. This value agrees with literature values for CHO, hybridoma, and BHK cells (Table 1-2).

The trend seen in the glucose-lactate yields make sense from a biological perspective. As oxygen levels drop, so does the oxygen driving force that powers the TCA cycle. As this cycle becomes less available, cells would have to switch to simple glycolysis as a source of ADP from glucose. If the TCA cycle is unavailable, pyruvate is shunted to lactate to regenerate the NADH needed to continue with glycolysis. Therefore a higher percentage of glucose would be converted to lactate, as is seen in the data from the first run. This same trend was also seen in myocytes (Silverman et. al., 1997), hybridoma (Ozturk & Pallson, 1990; Europa et. al., 2000), and murine embryonic cells (Sanford et. al., 1970).

Another important consideration is whether it is reasonable to assume that the glucose concentration remains high enough for its consumption to be constant. Glucose consumption has been shown to exhibit Michaelis-Menten kinetics in hybridoma cells where the consumption rate was constant at glucose concentrations above 0.22 g/L. (Cruz et. al., 1999). Nearly all of the glucose concentrations measured were above 1 g/L, so it is probably

reasonable to assume that glucose consumption is linear, as long as metabolism in stem cells is not dramatically different from metabolism in hybridoma cells.

4.4 Amino acid metabolism

A thorough treatment of glutamine metabolism was done by Petch and Butler (1994), where they traced metabolic pathways in hybridoma cells. Their findings are summarized in Table 1-1. One important observation is that very little glutamine is converted to glutamate as an end product. This finding suggests that glutamate acts as more of a transition metabolite before it produces either ammonia or alanine and enters the TCA cycle. Since ammonia is also produced in the conversion of glutamine to glutamate, glutamine to ammonia yield is probably more indicative of the metabolic state of the cell than glutamine to glutamate yield. Since carbon dioxide is a common end product of glutamine metabolism in hybridoma, this could be contributing to the observation that evaporation occurs at a higher rate when cell growth is occurring.

Glutamine is a key metabolite in cell culture, as the consumption rate of glutamine is typically about an order of magnitude higher than the other amino acids (Wang et. al., 2002). Ammonia is a byproduct of glutamine metabolism, and the amount of ammonia produced is indicative of the pathways being utilized. Ammonia can be dangerous to cells, as it is an order of magnitude more toxic than lactate. Hybridoma cells have been shown to die at ammonia concentrations higher than 7.8 mM. (Cruz et. al., 2000). Fortunately for the health of the cells, and unfortunately for the purpose of doing metabolic calculations, ammonia evaporates from cell culture medium at an appreciable rate. Nine percent of added ammonium was found to evaporate in 72 hours from 6-well plates (Lao & Toth, 1997). Like glucose, glutamine consumption follows Michaelis-Menten kinetics. However, in hybridoma cells, glutamine to ammonia yield has been shown to be constant as long as the glutamine concentration was above 0.3mM (Cruz et. al., 1999). The majority of glutamine concentrations measured for stem cell metabolism were above 1 mM, so it seems reasonable to assume that glutamine-ammonia yields measured in this study should be more or less constant within each run. The calculated glutamine-ammonia yield was 0.19 mol/mol, which is 27% of the values reported in the literature for hybridoma, BHK, and CHO cells (Table 1-2). A large part of this

discrepancy is probably due to the evaporation of ammonia from the system due to the convective gas flow across the top of the plates. Future work should account for not only evaporation of medium, but also evaporation of ammonia. While evaporation of ammonia was probably good for the health of the cells, it makes it impossible to know how accurate the glutamine-ammonia yield was.

While there is no strong trend that can be seen in the data, it appears that glutamine-ammonia yield is higher at intermediate oxygen concentrations, and lower at the extremes. The second run data point is interesting because it suggests that ammonia and glutamine are both consumed during cell culture. This odd result is probably due to the low metabolic rate of the cells during that run. Since all the data points were compressed into less than 55 hours, there was very little metabolism that occurred relative to the first set of metabolism and kinetics experiments. It's entirely possible that the sign on this yield is different because the evaporation rate of ammonia is higher than the rate it is being produced. All the yields from the second run are lower probably due to this effect. In the first run, the glutamine level changed less during the 2%, 5%, and 10% runs than during the 0% and 20% runs. This implies that ammonia production should be lower, and that ammonia evaporation would have a greater effect on the yields measured between 2% and 10%. However, the yields are actually higher than the yields at 0% and 20% in spite of the evaporation occurring. These higher yields could be indicative of a different mode of glutamine metabolism at intermediate oxygen levels. Glutamine can be converted into α-ketoglutarate via two different pathways: one that yields one ammonia molecule, and a second that yields two ammonia molecules. (Figure 1-3) The pathway that produces two ammonia molecules is more energetically efficient, so the higher glutamine-ammonia yields could be indicative of a more efficient mode of glutamine metabolism at intermediate oxygen concentrations.

4.5 Utilization of glucose vs glutamine

In the first run at atmospheric conditions, glucose was used at a rate of 0.22×10^6 cells/gram, and glutamine was used at a rate of 1.2×10^6 cells/gram. Looking at literature values in Table 1-2, it can be seen that stem cells are considerably less efficient than BHK, CHO, and hybridoma cells at converting glucose and glutamine to cells. While part of the difference

could be due to a difference in cell size, this would not be sufficient to explain the difference of three orders of magnitude. One possible explanation for the 3 order of magnitude discrepancy in yields is the high rate at which stem cells multiply compared to other cells because stem cells lack a G1 checkpoint. The constant cell division may shift the cells into some sort of metabolic overdrive resulting in a reduced cellular yield. It is also interesting to note that glutamine is used much more efficiently (by nearly an order of magnitude in some cases) than glucose from a biomass perspective. However, glucose is present at a much higher concentration than glutamine in stem cell medium. Glucose may be used less efficiently simply because more is available. The probability of correlation of glucose to cell yield was high for both runs (above 95%), and the glutamine-cell yields were more than 70% likely to be correlated with oxygen concentration for both runs. These correlations suggest that stem cell metabolism is less efficient at low oxygen concentrations, which makes sense from a biological perspective. As oxygen levels drop, the cell is less able to use more efficient oxidative metabolic processes, and it shifts towards less efficient anaerobic processes.

4.6 Plating efficiency

No obvious conclusions can be drawn from the data depicted in Figure 3-3. If there is a correlation in the data, it is a weak one, as there is a less than 50% probability that the data are correlated. Because much stronger conclusions could be drawn from the metabolism and kinetics data, plans to repeat the plating efficiency trials several more times were abandoned. Improvements in plating efficiency have been reported in the literature (Wiles, 1993; Potocnik et. al., 1994; Gassmann et. al., 1996), and support the hypothesis that stem cells are better suited for growing in a mildly hypoxic environment.

5 Conclusion

Several interesting conclusions can be drawn from the data collected in this experiment. The most significant finding was that medium evaporation can have a significant impact on metabolic yield calculations, and should not be neglected as is commonly done in metabolic studies. As expected, stem cells grew faster in a hypoxic environment than they did in atmospheric conditions, where the doubling time was as much as 32% lower. However, dropping the oxygen concentration below 2% is counterproductive, as it makes cellular doubling time up to 44% longer than at atmospheric conditions. The maximum sustainable cell density (12.29 x 10^6 cells/6 cm plate at atmospheric conditions) decreased as oxygen supply decreased and caused the cells to shift into a more anaerobic mode of glucose metabolism. In this less efficient metabolic mode, pyruvate is converted to lactate to regenerate the NADH required for gylcolysis to continue. As a result of this shift, the yield of glucose to lactate increased as oxygen concentration decreased. Furthermore, glutamine and glucose were used progressively less efficiently for producing cell mass as the oxygen concentration decreased from 20% to 0%. No strong trends could be observed for the glutamine-ammonia yield, although it appears that more ammonia may be produced per glutamine when the oxygen concentration is between 2% and 10%. Evaporation of ammonia likely caused all of the reported yields to be lower than the true yields. Since the evaporation rate of ammonia in the system was not known, it was impossible to estimate the true yields. Although plating efficiency has been shown to increase as oxygen concentration decreases in other studies, this study did not find any correlation between the two parameters, although one could become apparent with more data. In terms of maximum sustainable cell density and metabolic efficiency, it is better to grow cells at a higher oxygen concentration. In terms of growth rate, it seems best to grow cells between 2% and 10% oxygen. Given these two constraints, it may be best to grow murine embryonic stem cells in a hypoxic environment with a headspace oxygen concentration of 10% by volume to take advantage of a higher growth rate while minimizing the cell density and metabolic efficiency losses. In environments where I is possible to control the oxygen levels throughout the run, it may be even more

efficient to start culturing cells in hypoxic conditions and switch to atmospheric conditions as the cells become confluent.

5.1 Future Work

Several questions brought up in the experiments of this study could be the subject of future work. Potential future experiments include:

- Measure apoptosis as a function of oxygen concentration as a means to determine the "health" of cells growing in hypoxic conditions relative to cells growing in atmospheric conditions.

- Perform assays to determine stem cell DNA damage as a function of oxygen concentration and compare the results to the level of DNA damage that occurs at atmospheric conditions.

- Repeat the experiments done in this study several times to determine how robust the results are.

- Look at the Michaelis-Menten kinetics of glucose and glutamine consumption in stem cells and compare to the kinetics observed in hybridoma, CHO, and BHK cells.

- Quantify the evaporation rate of ammonia from cell culture medium to "correct" glutamine-ammonia yield values.

- Measure the medium evaporation rate when cells are present and compare to the cell-free evaporation rate.

APPENDICES

A Calculations

A.1 Linear Regression (Taylor 1997)

Given data points $(x_1, y_1), (x_2, y_2) \ldots (x_n, y_n)$, the slope and intercept of the best-fit line passing through these points are given by:

$$Slope = \frac{n\sum_{i=1}^{n} x_i y_i - \sum_{i=1}^{n} x_i \sum_{i=1}^{n} y_i}{n\sum_{i=1}^{n} x_i^{\,2} - \left(\sum_{i=1}^{n} x_i\right)^2}$$

$$Intercept = \frac{\sum_{i=1}^{n} x_i^{\,2} \sum_{i=1}^{n} y_i - \sum_{i=1}^{n} x_i \sum_{i=1}^{n} x_i y_i}{n\sum_{i=1}^{n} x_i^{\,2} - \left(\sum_{i=1}^{n} x_i\right)^2}$$

The uncertainty in the y_i measurements can then be calculated:

$$\sigma_y = \sqrt{\frac{1}{N-2}\sum_{i=1}^{n}\left(y_i - Intercept - Slope \cdot x_i\right)^2}$$

The σ_y can now be used to calculate the standard error of the regression slope and intercept:

$$\sigma_{Slope} = \sigma_y \sqrt{\frac{\sum_{i=1}^{n} x_i^{\,2}}{n\sum_{i=1}^{n} x_i^{\,2} - \left(\sum_{i=1}^{n} x_i\right)^2}}$$

$$\sigma_{Intercept} = \sigma_y \sqrt{\frac{n}{n\sum_{i=1}^{n} x_i^{\,2} - \left(\sum_{i=1}^{n} x_i\right)^2}}$$

A.2 Weighted Linear Regression (Taylor 1997)

When there are error bars on the regression data points, it is better to use a weighted linear regresson so that points with greater certainty are given more weight. If error is limited to the y coordinate (or if error in x is negligible compared to error in y), σ_i is simply equal to the error in y_i. If error is in both coordinates, a more complicated approach must be taken. Since a line is being fit through the data points, an error in x is equal to an equivalent error in y. The total error can then be found with:

$$\sigma_{y,equiv} = \sqrt{\sigma_y^{\,2} + (Slope \cdot \sigma_x)^2}$$

Since the slope is not yet known, this value must be approximated before the weighted regression can be done. Iteration can then be used to find the correct slope. A MAPLE procedure for this iteration can be found in Appendix B. Once the values of σ_i are known, the corresponding weights can be calculated:

$$w_i = \frac{1}{\sigma_i^{\,2}}$$

The weights for each data point are then used to calculate the regression slope and intercept:

$$Slope = \frac{\sum_{i=1}^{n} w_i \sum_{i=1}^{n} w_i x_i y_i - \sum_{i=1}^{n} w_i x_i \sum_{i=1}^{n} w_i y_i}{\sum_{i=1}^{n} w_i \sum_{i=1}^{n} w_i x_i^{\,2} - \left(\sum_{i=1}^{n} w_i x_i\right)^2}$$

$$Intercept = \frac{\sum_{i=1}^{n} w_i x_i^{\,2} \sum_{i=1}^{n} w_i y_i - \sum_{i=1}^{n} w_i x_i \sum_{i=1}^{n} w_i x_i y_i}{\sum_{i=1}^{n} w_i \sum_{i=1}^{n} w_i x_i^{\,2} - \left(\sum_{i=1}^{n} w_i x_i\right)^2}$$

Standard error of the slope and intercept can then be calculated:

$$\sigma_{Slope} = \sqrt{\frac{\sum_{i=1}^{n} w_i x_i^2}{\sum_{i=1}^{n} w_i \sum_{i=1}^{n} w_i x_i^2 - \left(\sum_{i=1}^{n} w_i x_i\right)^2}}$$

$$\sigma_{Intercept} = \sqrt{\frac{\sum_{i=1}^{n} w_i}{\sum_{i=1}^{n} w_i \sum_{i=1}^{n} w_i x_i^2 - \left(\sum_{i=1}^{n} w_i x_i\right)^2}}$$

A.3 Comparing Regression Slopes

Sometimes regression slopes need to be compared to see if they are statistically different. A procedure is outlined by Jerold H. Zar in his text *Biostatistial Analysis* (Zar 1996). The comparison is done between two data sets (i = 1 and i = 2). The information needed from each set are the x values (X_i), the y values (Y_i), the number of data points (n_i), and the regression slope ($Slope_i$).

A few definitions simplify the calculations:

$$\sum x_i^2 \equiv \sum_{j=1}^{n_i} X_i^2 - \frac{1}{n_i}\left(\sum_{j=1}^{n_i} X_i\right)^2$$

$$\sum x_i y_i \equiv \sum_{j=1}^{n_i} X_i Y_i - \frac{1}{n_i}\sum_{j=1}^{n_i} X_i \sum_{j=1}^{n_i} Y_i$$

$$\sum y_i^2 \equiv \sum_{j=1}^{n_i} Y_i^2 - \frac{1}{n_i}\left(\sum_{j=1}^{n_i} Y_i\right)^2$$

The t-value can then be calculated:

$$t = \frac{\left|Slope_1 - Slope_2\right|}{\sqrt{\left(\frac{\sum y_1^{\,2} - \frac{\left(\sum x_1 y_1\right)^2}{\sum x_1^{\,2}} + \sum y_2^{\,2} - \frac{\left(\sum x_2 y_2\right)^2}{\sum x_2^{\,2}}}{n_1 + n_2 - 4}\right)\left(\frac{1}{\sum x_1^{\,2}} + \frac{1}{\sum x_2^{\,2}}\right)}}$$

Degrees of freedom for the t-test are:

$$\nu = n_1 + n_2 - 4$$

Student's t-distribution is given by (Maple Docs):

$$t_{dist} = \frac{\Gamma\left(\frac{\nu+1}{2}\right)}{\Gamma\left(\frac{\nu}{2}\right)\sqrt{\nu\pi}\left(1 + \frac{t^2}{\nu}\right)^{\left(\frac{\nu+1}{2}\right)}}$$

The probability that the difference in means is statistically significant can be found by integrating the t-distribution:

$$p\left(slope_1 \neq slope_2\right) = \int_{t=-t}^{t=t} t_{dist}\, dt$$

A.4 Correlation (Taylor 1997)

Another useful calculation is to determine the probability that two variables are correlated. The r value is given by:

$$r = \frac{\sum (x_i - \bar{x})(y_i - \bar{y})}{\sqrt{\sum (x_i - \bar{x})^2 \sum (y_i - \bar{y})^2}}$$

where x_i and y_i are the data points, and $\bar{x}$ and $\bar{y}$ are the means.

The probability that the variables are not correlated is:

$$p(|r| \geq |r_o|) = \frac{2\Gamma\left(\frac{N-1}{2}\right)}{\sqrt{\pi}\Gamma\left(\frac{N-2}{2}\right)} \int_{|r_o|}^{1} \left(1-r^2\right)^{\frac{N-4}{2}} dr$$

A.5 Calculating Doubling Times

Doubling time can be calculated from the equations given in Section 1.5:

$$t_d = \frac{\ln 2}{\mu}$$

Since the standard error of the linear regression is the error of μ, the error of the doubling time must be found via error propagation:

$$\Delta t_d = \frac{\Delta\mu \ln 2}{\mu^2}$$

A.6 Calculating ammonia concentrations

The Nova Bioprofiler measures pH and $[NH_4^+]$. These two values can be used to calculate the ammonia concentration NH_3 with the Henderson-Hasselbalch Equation:

$$pH = pK_a + \log_{10}\left(\frac{[NH_3]}{[NH_4^+]}\right)$$

This equation can be rearranged to give the total ammonia concentration (ionic and neutral):

$$[NH_3] + [NH_4^+] = [NH_4^+]\left(1 + 10^{pH-pK_a}\right)$$

The pK_a of ammonia is 9.23.

B Curve Fits

B.1 Rotameter Calibration

Calibration data for the rotameter used is given below:

rotameter reading	calibrated value (cc/min)
150	250
91.5	125
120	200
40	40
10	14

Table 5-1: Rotameter calibration values. Rotameter was calibrated using an Alltech Direct Reading Flow Check (#7080)

A polynomial was fit through the data points for interpolation:

$$y = -2.0392x10^{-6}x^4 + 5.5732E\text{-}04x^3 - .038558x^2 + 1.7975x - 0.65649$$

B.2 BioProfiler pH

The final three data points of the first 2% oxygen run had a pH that the BioProfiler was unable to calculate. To estimate the pH of these values, the pH before freezing was compared to the pH measured by the BioProfiler after thawing down the samples for analysis. A line was fit through the data points to estimate the value of the missing post-thaw pH measurements.

pre-thaw	post-thaw
7.67	8.782
7.75	8.253
7.80	8.136
7.46	7.728
7.51	7.702
7.52	7.681
6.71	7.103
6.69	7.08
6.71	7.093

Table 5-2: Correlation of pH before and after thawing samples

Slope was found to be 1.100795, and the intercept was found to be -0.32181.

C Contamination in convective evaporation experiment

	Mass (g)					Slope	Comparison
Time(h)	*22.85*	*40.18*	*47.27*	*56.73*	*70.95*	(g/h)	%
1	7.3385	7.2050	7.0556	6.9194	6.7830	-0.0121	N/A
2	7.6304	7.5180	7.3963	7.2713	7.1445	-0.0106	1
3	7.4366	7.3282	7.2100	7.0888	6.9653	-0.0103	71
4	7.3815	7.2670	7.1523	7.0246	6.9032	-0.0104	N/A
5	7.4205	7.2936	7.1529	7.0100	6.8845	-0.0118	16
6	7.4030	7.2886	7.1758	7.0581	6.9379	-0.0101	N/A
7	7.3431	7.2406	7.1343	7.0180	6.9017	-0.0096	70
8	7.5200	7.4281	7.3380	7.2222	7.1151	-0.0088	N/A
9	7.2911	7.1663	7.0259	6.8750	6.7496	-0.0119	58
10	7.2760	7.1636	7.0567	6.9321	6.8152	-0.0100	63
11	7.5678	7.4542	7.3496	7.2278	7.1063	-0.0100	N/A
12	7.1645	7.0483	6.9510	6.8237	6.7043	-0.0100	N/A
13	7.3284	7.1975	7.0835	6.9000	6.7904	-0.0119	N/A
14	7.5837	7.4595	7.3547	7.2204	7.1013	-0.0105	57
15	7.3798	7.2437	7.1290	6.9895	6.5631	-0.0166	74

Table 5-3: Evaporation rate as a function of plate position and presence of contamination

	1	**2**	**3**	**4**	**5**	**6**	**7**	**8**	**9**	**10**	**11**	**12**	**13**	**14**	**15**
1	0	68	77	73	18	82	89	80	11	83	84	84	57	73	79
2	68	0	18	10	55	29	53	80	59	33	35	37	57	6	90
3	77	18	0	9	66	10	39	72	69	15	16	18	67	14	91
4	73	10	9	0	62	20	47	77	33	24	26	28	63	4	91
5	18	55	66	62	0	73	100	92	7	74	75	76	7	61	82
6	82	29	10	20	73	0	31	69	75	5	6	8	73	25	92
7	89	53	39	47	100	31	0	47	84	27	26	24	82	52	94
8	**80**	**80**	**72**	**77**	**92**	**69**	**47**	**0**	**93**	**66**	**66**	**65**	**91**	**80**	**96**
9	11	59	69	33	7	75	84	93	0	76	77	78	0	64	81
10	83	33	15	24	74	5	27	66	76	0	1	4	74	29	92
11	84	35	16	26	75	6	26	66	77	1	0	2	75	31	92
12	84	37	18	28	76	8	24	65	78	4	2	0	76	33	93
13	57	57	67	63	7	73	82	91	0	74	75	76	0	62	81
14	73	6	14	4	61	25	52	80	64	29	31	33	62	0	91
15	79	90	91	91	82	92	94	96	81	92	92	93	81	91	0

Table 5-4: Probability that differences in evaporation rates between plates are statistically significant. The darkened row is the plate in which no contamination appeared.

D MAPLE Source Code

```
Thesis := module()
  description "Analysis routines for thesis data";
  export LSquares, Compare, p_corr, Regress, Regress2, Compare5;
  local Ttest, Newton;
  option package;

 Newton := proc(Eqn, x, x0)
 local newx,i,m;

 newx := x0;

 for i from 1 to 20 do
   m := subs(x=newx,diff(Eqn,x));
   newx := (m*newx-subs(x=newx,Eqn))/m;
 end do;

 end proc:

 Regress := proc(x,y)

  local X, Y, n, Delta, sigma,
       SLOPE, dSLOPE, INTERCEPT, dINTERCEPT,
       Sxx, Sx, Sy, Sxy;

  X := Vector([flatten(x)]); Y := Vector([flatten(y)]);

  n := nops([flatten(X)]);

  Sxx := sum('X[i]*X[i]',i = 1..n);
  Sx := sum('X[i]',i = 1..n);
  Sxy := sum('X[i]*Y[i]',i = 1..n);
  Sy := sum('Y[i]',i = 1..n);
  Delta := n*Sxx-Sx^2;
  SLOPE := (1/Delta)*(n*Sxy-Sx*Sy);
  INTERCEPT := (1/Delta)*(Sxx*Sy-Sx*Sxy);
  sigma := sqrt((1/(n-2))*sum('(Y[i]-INTERCEPT-SLOPE*X[i])^2',i=1..n));
  dSLOPE := sigma*sqrt(n/Delta);
  dINTERCEPT := sigma*sqrt(Sxx/Delta);
  evalf([SLOPE,dSLOPE,INTERCEPT,dINTERCEPT])

  end proc:

 Regress2 := proc(x1,y1,x2,y2)

   local X1, Y1, X2, Y2, n1, n2,
        SLOPE1, SLOPE2, t, p, Sx1, Sy1, Sxy1, Sx2, Sy2, Sxy2;

   X1 := Vector([flatten(x1)]); Y1 := Vector([flatten(y1)]);
   X2 := Vector([flatten(x2)]); Y2 := Vector([flatten(y2)]);

   n1 := nops([flatten(X1)]);
   n2 := nops([flatten(X2)]);
```

```
  Sx1 := sum('X1[i]^2',i = 1..n1)-(1/n1)*sum('X1[i]',i = 1..n1)^2;
  Sxy1:= sum('X1[i]*Y1[i]',i = 1..n1)-(1/n1)*
           sum('X1[i]',i = 1..n1)*sum('Y1[i]',i = 1..n1);
  Sy1 := sum('Y1[i]^2',i = 1..n1)-(1/n1)*sum('Y1[i]',i = 1..n1)^2;

  Sx2 := sum('X2[i]^2',i = 1..n2)-(1/n2)*sum('X2[i]',i = 1..n2)^2;
  Sxy2 := sum('X2[i]*Y2[i]',i = 1..n2)-(1/n2)*
           sum('X2[i]',i = 1..n2)*sum('Y2[i]',i = 1..n2);
  Sy2 := sum('Y2[i]^2',i = 1..n2)-(1/n2)*sum('Y2[i]',i = 1..n2)^2;

  SLOPE1 := Sxy1/Sx1;
  SLOPE2 := Sxy2/Sx2;

  t := abs((SLOPE1-SLOPE2)/sqrt(((Sy1-Sxy1^2/Sx1+Sy2-Sxy2^2/Sx2)/
           (n1+n2-4))*(1/Sx1+1/Sx2)));
  p := stats[statevalf,cdf,studentst[n1+n2-4]](t) -
           stats[statevalf,cdf,studentst[n1+n2-4]](-t);

  100*p;

  end proc:

LSquares := proc(x,y,dx,dy)

 local X, Y, dX, dY,
      sigma, n, Delta,
      SLOPE, dSLOPE, INTERCEPT, dINTERCEPT,
      S, Sxx, Sx, Sy, Sxy, SLOPE0,
      Equation;

 X := Vector(x); Y := Vector(y); dX := Vector(dx); dY := Vector(dy);

 n := nops([flatten(X)]);

 # Assume all error is in y for initial guess
 sigma := dY;
 S := sum('1/(sigma[i]^2)',i = 1..n);
 Sxx := sum('X[i]^2/(sigma[i]^2)',i = 1..n);
 Sx := sum('X[i]/(sigma[i]^2)',i = 1..n);
 Sy := sum('Y[i]/(sigma[i]^2)',i = 1 .. n);
 Sxy := sum('X[i]*Y[i]/(sigma[i]^2)',i = 1 .. n);
 Delta := S*Sxx-Sx^2;
 SLOPE0 := 1/Delta*(S*Sxy-Sx*Sy);

 # Iterate to find true slope
 sigma := zip((dx, dy)->sqrt((SLOPE*dx)^2+dy^2),dX,dY);
 S := sum('1/(sigma[i]^2)',i = 1..n);
 Sxx := sum('X[i]^2/(sigma[i]^2)',i = 1..n);
 Sx := sum('X[i]/(sigma[i]^2)',i = 1..n);
 Sy := sum('Y[i]/(sigma[i]^2)',i = 1..n);
 Sxy := sum('X[i]*Y[i]/(sigma[i]^2)',i = 1..n);
 Delta := S*Sxx-Sx^2;
 Equation := 1/Delta*(S*Sxy-Sx*Sy)-SLOPE;
```

```
  SLOPE := Newton(Equation, SLOPE, SLOPE0);

  # Calculate parameter values
  sigma := zip((dx, dy)->sqrt((SLOPE*dx)^2+dy^2),dX,dY);
  S := sum('1/(sigma[i]^2)',i = 1..n);
  Sxx := sum('X[i]^2/(sigma[i]^2)',i = 1..n);
  Sx := sum('X[i]/(sigma[i]^2)',i = 1..n);
  Sy := sum('Y[i]/(sigma[i]^2)',i = 1 .. n);
  Sxy := sum('X[i]*Y[i]/(sigma[i]^2)',i = 1 .. n);
  Delta := S*Sxx-Sx^2;
  INTERCEPT := 1/Delta*(Sxx*Sy-Sx*Sxy);
  dINTERCEPT := sqrt(Sx/Delta);
  dSLOPE := sqrt(S/Delta);

  evalf([SLOPE,dSLOPE,INTERCEPT,dINTERCEPT])

  end proc:


 Ttest := proc(m1,m2,s1,s2,n1,n2)
   local t;
   t := (m1-m2)/sqrt(s1^2/n1+s2^2/n2):
   stats[statevalf,cdf,studentst[n1+n2-2]](t)-
stats[statevalf,cdf,studentst[n1+n2-2]](-t)
 end proc:

  Compare5 := proc(x1,y1,x2,y2,x3,y3,x4,y4,x5,y5)
   local TMatrix,n,X1,X2,X3,X4,X5,Y1,Y2,Y3,Y4,Y5,N1,N2,N3,N4,N5,X;

     X1 := [flatten(x1)];
     X2 := [flatten(x2)];
     X3 := [flatten(x3)];
     X4 := [flatten(x4)];
     X5 := [flatten(x5)];

     Y1 := [flatten(y1)];
     Y2 := [flatten(y2)];
     Y3 := [flatten(y3)];
     Y4 := [flatten(y4)];
     Y5 := [flatten(y5)];

     N1 := nops(X1);
     N2 := nops(X2);
     N3 := nops(X3);
     N4 := nops(X4);
     N5 := nops(X5);

     n := 5;
     TMatrix := Matrix(n,n);

     TMatrix[1,1] := X;
     TMatrix[1,2] := (Regress2(X1,Y1,X2,Y2));
     TMatrix[1,3] := (Regress2(X1,Y1,X3,Y3));
     TMatrix[1,4] := (Regress2(X1,Y1,X4,Y4));
```

```
    TMatrix[1,5] := (Regress2(X1,Y1,X5,Y5));
    TMatrix[2,1] := (Regress2(X1,Y1,X2,Y2));
    TMatrix[2,2] := X;
    TMatrix[2,3] := (Regress2(X3,Y3,X2,Y2));
    TMatrix[2,4] := (Regress2(X4,Y4,X2,Y2));
    TMatrix[2,5] := (Regress2(X5,Y5,X2,Y2));
    TMatrix[3,1] := (Regress2(X1,Y1,X3,Y3));
    TMatrix[3,2] := (Regress2(X3,Y3,X2,Y2));
    TMatrix[3,3] := X;
    TMatrix[3,4] := (Regress2(X3,Y3,X4,Y4));
    TMatrix[3,5] := (Regress2(X3,Y3,X5,Y5));
    TMatrix[4,1] := (Regress2(X1,Y1,X4,Y4));
    TMatrix[4,2] := (Regress2(X4,Y4,X2,Y2));
    TMatrix[4,3] := (Regress2(X4,Y4,X3,Y3));
    TMatrix[4,4] := X;
    TMatrix[4,5] := (Regress2(X4,Y4,X5,Y5));
    TMatrix[5,1] := (Regress2(X1,Y1,X5,Y5));
    TMatrix[5,2] := (Regress2(X5,Y5,X2,Y2));
    TMatrix[5,3] := (Regress2(X5,Y5,X3,Y3));
    TMatrix[5,4] := (Regress2(X4,Y4,X5,Y5));
    TMatrix[5,5] := X;

    TMatrix

  end proc:

 p_corr := proc(N,Ro)
     evalf(2*GAMMA((N-1)/2)/(sqrt(Pi)*GAMMA((N-2)/2))*
           int((1-r^2)^((N-4)/2),r=abs(Ro)..1))
 end proc:

end module:
```

E Raw Data

E.1 Reaction Vessel Metabolism and Kinetics

	0%: Run 1		1-1	1-2	1-3	2-1	2-2	2-3	3-1	3-2	3-3	4-1	4-2	4-3	5-1	5-2	5-3
	Time	(hours)	1565	1565	1565	2505	2505	2505	3180	3180	3180	3920	3920	3920	4375	4375	4375
Nova Bioanalyzer	*pH*		*8.294*	*8.308*	*8.279*	*8.051*	*8.115*	*8.090*	*7.772*	*7.796*	*7.814*	*7.316*	*7.397*	*7.329*	*7.093*	*7.105*	*7.070*
	Gln	*(mM)*	*1.22*	*1.51*	*1.40*	*1.27*	*1.37*	*1.36*	*1.29*	*1.25*	*1.17*	*1.31*	*1.17*	*1.25*	*1.20*	*1.24*	*1.20*
	Glu	*(mM)*	*0.37*	*0.38*	*0.35*	*0.36*	*0.38*	*0.40*	*0.32*	*0.40*	*0.40*	*0.52*	*0.48*	*0.44*	*0.42*	*0.42*	*0.39*
	Gluc	*(g/L)*	*2.46*	*2.63*	*2.46*	*2.04*	*2.26*	*2.25*	*1.78*	*1.73*	*1.56*	*1.29*	*1.34*	*1.30*	*1.10*	*1.18*	*1.11*
	Lac	*(g/L)*	*0.73*	*0.97*	*0.95*	*1.20*	*1.29*	*1.26*	*1.57*	*1.70*	*1.64*	*2.27*	*2.11*	*2.14*	*2.10*	*2.20*	*2.15*
	NH4+	*(mM)*	*0.49*	*0.49*	*0.48*	*0.43*	*0.58*	*0.55*	*0.64*	*0.73*	*0.57*	*0.98*	*0.87*	*0.89*	*0.86*	*0.87*	*0.97*
	Na+	*(mM)*	*105.2*	*113.9*	*108.1*	*108.2*	*117.9*	*121.2*	*123.9*	*119.7*	*124.4*	*140.8*	*135.6*	*129.4*	*120.8*	*132.9*	*130.5*
	K+	*(mM)*	*4.49*	*4.74*	*4.56*	*4.55*	*4.89*	*5.00*	*5.06*	*4.94*	*5.08*	*5.66*	*5.44*	*5.30*	*5.06*	*5.42*	*5.40*
	Osm	*(mOsm/kg)*	*286.7*	*306.9*	*294.6*	*295.2*	*316.3*	*322.2*	*328.4*	*321.7*	*328.8*	*366.6*	*354.8*	*343.2*	*325.1*	*349.9*	*344.6*
Cedex/YSI/pH/HPLC	Pyr	(mg/L)	77.95	75.78	78.57	59.98	62.67	62.43	51.88	49.90	49.52	45.94	38.74	44.17	41.97	43.64	42.94
	Gluc	(g/L)	3.59	3.53	3.51	2.91	3.05	3.03	2.34	2.11	2.10	1.58	1.59	1.58	1.26	1.33	1.29
	Lac	(g/L)	0.738	0.803	0.758	1.41	1.45	1.39	2.03	2.17	2.26	3.33	3.06	3.29	3.18	3.30	3.45
	Gln	(mM)	3.160	3.340	3.060	2.05	3.29	2.26	2.73	2.66	2.33	2.89	2.42	1.95	1.88	2.31	1.78
	Glu	(mM)	0.632	0.616	0.707	0.50	0.71	0.46	0.61	0.64	0.51	0.76	0.61	0.43	0.42	0.58	0.49
	pH		7.90	7.98	7.98	7.75	7.80	7.92	7.67	7.55	7.54	6.97	7.12	7.14	6.68	6.68	6.60
	VCD	(10^5 cells/mL)	3.51	4.21	3.54	6.17	6.66	5.89	10.04	11.42	11.20	12.48	10.44	12.20	11.33	11.30	11.19
	Via	(%)	97.5	97.9	96.3	99.1	96.8	97.0	98.7	96.5	96.6	96.2	94.7	93.4	94.0	92.6	92.5

	2%: Run 1		1-1	1-2	1-3	2-1	2-2	2-3	3-1	3-2	3-3	4-1	4-2	4-3
	Time	(hours)	1240	1240	1240	1950	1950	1950	2605	2605	2605	3845	3845	3845
Nova Bioanalyzer	*pH*		*8.782*	*8.253*	*8.136*	*7.728*	*7.702*	*7.681*	*7.103*	*7.080*	*7.093*			
	Gln	*(mM)*	*1.12*	*1.23*	*1.56*	*1.17*	*1.11*	*1.12*	*1.00*	*0.87*	*0.93*	*0.78*	*0.84*	*1.02*
	Glu	*(mM)*	*0.48*	*0.34*	*0.41*	*0.42*	*0.41*	*0.29*	*0.44*	*0.38*	*0.41*	*0.42*	*0.53*	*0.44*
	Gluc	*(g/L)*	*2.12*	*2.12*	*2.80*	*1.69*	*1.58*	*1.49*	*0.99*	*0.94*	*0.93*	*0.74*	*0.80*	*0.89*
	Lac	*(g/L)*	*1.02*	*1.07*	*1.37*	*2.23*	*2.06*	*2.10*	*2.50*	*2.43*	*2.35*	*2.58*	*2.65*	*2.86*
	NH4+	*(mM)*	*0.32*	*0.42*	*0.56*	*0.76*	*0.74*	*0.75*	*0.92*	*0.91*	*0.90*	*1.02*	*1.10*	*1.19*
	Na+	*(mM)*	*98.3*	*95.8*	*118.8*	*124.9*	*114.4*	*124.9*	*113.7*	*113.9*	*108.6*	*109.6*	*117.9*	*130.0*
	K+	*(mM)*	*4.18*	*4.12*	*4.85*	*4.96*	*4.68*	*4.94*	*4.63*	*4.62*	*4.50*	*4.64*	*4.93*	*5.41*
	Osm	*(mOsm/kg)*	*274.3*	*270.3*	*321.8*	*337.1*	*314.5*	*334.5*	*315.1*	*314.3*	*303.3*	*307.1*	*324.4*	*350.8*
Cedex/YSI/pH/HPLC	Pyr	(mg/L)	63.60	73.01	73.43	50.42	50.87	57.87	44.56	45.30	47.25	33.72	35.35	37.28
	Gluc	(g/L)	2.89	2.95	2.94	1.79	1.80	1.76	1.11	1.11	1.16	0.84	0.91	0.91
	Lac	(g/L)	1.180	1.170	1.140	2.28	2.30	2.42	3.14	3.23	3.53	3.27	3.65	3.75
	Gln	(mM)	3.080	2.360	1.560	1.13	2.29	1.52	1.74	1.02	1.38	1.32	1.58	1.41
	Glu	(mM)	0.622	0.443	0.292	0.24	0.54	0.36	0.47	0.26	0.38	0.40	0.48	0.38
	pH		7.67	7.75	7.80	7.46	7.51	7.52	6.71	6.69	6.71	6.17	6.17	6.09
	VCD	(10^5 cells/mL)	12.46	12.67	12.59	25.07	22.34	24.69	30.42	29.42	28.68	15.72	16.07	8.12
	Via	(%)	95.8	95.4	96.2	98.0	98.2	97.2	97.3	96.3	95.7	69.0	65.9	58.2

	5%: Run 1		1-1	1-2	1-3	2-1	2-2	2-3	3-1	3-2	3-3	4-1	4-2	4-3	5-1	5-2	5-3
	Time	(hours)	1305	1305	1305	2230	2230	2230	2635	2635	2635	3390	3390	3390	4105	4105	4105
Nova Bioanalyzer	*pH*		*8.365*	*8.533*	*8.438*	*8.233*	*8.405*	*8.404*	*8.439*	*8.272*	*8.320*	*7.560*	*7.542*	*7.570*	*7.280*	*7.245*	*7.236*
	Gln	*(mM)*	*1.80*	*1.68*	*1.83*	*1.69*	*1.51*	*1.63*	*1.35*	*1.31*	*1.41*	*0.96*	*1.11*	*0.97*	*0.73*	*0.72*	*0.93*
	Glu	*(mM)*	*0.34*	*0.35*	*0.32*	*0.41*	*0.38*	*0.42*	*0.34*	*0.45*	*0.35*	*0.43*	*0.39*	*0.38*	*0.39*	*0.40*	*0.35*
	Gluc	*(g/L)*	*3.09*	*2.86*	*3.02*	*2.73*	*2.54*	*2.66*	*2.06*	*2.10*	*2.31*	*1.22*	*1.36*	*1.22*	*0.91*	*0.99*	*1.06*
	Lac	*(g/L)*	*0.53*	*0.59*	*0.68*	*1.36*	*1.24*	*1.30*	*1.59*	*1.62*	*1.52*	*2.63*	*2.70*	*2.56*	*2.66*	*2.86*	*2.79*
	NH4+	*(mM)*	*0.29*	*0.25*	*0.27*	*0.36*	*0.36*	*0.41*	*0.35*	*0.45*	*0.46*	*0.76*	*0.79*	*0.78*	*0.87*	*0.95*	*1.00*
	Na+	*(mM)*	*121.0*	*109.4*	*120.3*	*130.2*	*123.2*	*125.8*	*124.5*	*123.1*	*127.5*	*133.2*	*138.0*	*132.1*	*134.7*	*136.7*	*135.1*
	K+	*(mM)*	*4.86*	*4.46*	*4.84*	*5.10*	*4.87*	*4.99*	*4.84*	*4.78*	*5.00*	*5.03*	*5.18*	*5.01*	*5.13*	*5.18*	*5.19*
	Osm	*(mOsm/kg)*	*317.7*	*294.7*	*317.6*	*342.6*	*326.7*	*333.2*	*330.3*	*328.3*	*337.0*	*354.5*	*365.3*	*351.7*	*356.3*	*362.9*	*359.7*
Cedex/YSI/pH/HPLC	Pyr	(mg/L)	86.69	87.02	89.01	81.35	81.98	87.44	71.21	74.74	80.59	60.10	60.26	57.85	48.61	47.97	48.59
	Gluc	(g/L)	3.53	3.61	3.59	2.87	3.00	3.03	2.58	2.47	2.76	1.38	1.35	1.36	1.12	1.08	1.10
	Lac	(g/L)	0.491	0.473	0.493	1.14	1.11	1.15	1.63	1.58	1.49	2.78	2.77	2.37	3.15	3.18	3.38
	Gln	(mM)	2.270	1.820	1.870	1.63	2.34	1.56	2.18	1.55	1.77	1.05	1.50	1.32	0.91	0.84	0.73
	Glu	(mM)	0.317	0.251	0.258	0.29	0.43	0.27	0.47	0.31	0.34	0.28	0.43	0.39	0.29	0.27	0 23
	pH		8.03	8.03	8.08	7.97	7.88	7.90	7.73	7.69	7.74	7.23	7.23	7.20	6.72	6.73	6.75
	VCD	(10^5 cells/mL)	4.88	4.02	4.39	14.04	11.94	12.96	21.31	20.42	16.30	38.72	35.78	36.41	39.99	35.76	36.20
	Via	(%)	96.8	93.4	92.8	97.4	95.8	94.4	97.4	96.8	95.1	96.8	96.4	95.7	95.6	94.9	94.4

	10%: Run 1		1-1	1-2	1-3	2-1	2-2	2-3	3-1	3-2	3-3	4-1	4-2	4-3	5-1	5-2	5-3
	Time	(hours)	1430	1430	1430	2250	2250	2250	2710	2710	2710	3735	3735	3735	4210	4210	4210
Nova Bioanalyzer	*pH*		*9.001*	*9.083*	*9.052*	*8.813*	*8.857*	*8.806*	*8.640*	*8.583*	*8.465*	*7.577*	*7.533*	*7.606*	*7.392*	*7.354*	*7.356*
	Gln	*(mM)*	*1.11*	*1.58*	*1.49*	*1.08*	*1.17*	*1.29*	*1.10*	*1.07*	*1.06*	*0.52*	*0.51*	*0.62*	*0.27*	*0.43*	*0.34*
	Glu	*(mM)*	*0.38*	*0.43*	*0.50*	*0.42*	*0.45*	*0.48*	*0.44*	*0.39*	*0.49*	*0.38*	*0.51*	*0.46*	*0.39*	*0.47*	*0.55*
	Gluc	*(g/L)*	*1.94*	*2.75*	*2.58*	*1.81*	*1.94*	*2.14*	*1.78*	*1.64*	*1.90*	*0.91*	*1.08*	*1.03*	*0.84*	*1.00*	*0.98*
	Lac	*(g/L)*	*0.43*	*0.81*	*0.75*	*0.99*	*1.07*	*1.10*	*1.31*	*1.35*	*1.50*	*2.03*	*2.05*	*2.35*	*2.19*	*1.99*	*2.02*
	NH4+	*(mM)*	*0.27*	*0.24*	*0.28*	*0.35*	*0.33*	*0.42*	*0.42*	*0.48*	*0.58*	*0.85*	*0.94*	*1.00*	*1.11*	*1.01*	*1.07*
	Na+	*(mM)*	*85.8*	*117.5*	*107.8*	*94.1*	*98.4*	*111.9*	*104.4*	*99.8*	*124.1*	*109.1*	*116.3*	*129.1*	*120.7*	*110.0*	*115.9*
	K+	*(mM)*	*3.77*	*4.83*	*4.55*	*4.05*	*4.21*	*4.65*	*4.38*	*4.19*	*4.95*	*4.36*	*4.54*	*4.97*	*4.80*	*4.45*	*4.67*
	Osm	*(mOsm/kg)*	*242.6*	*312.2*	*292.1*	*264.2*	*271.1*	*301.7*	*287.5*	*278.4*	*328.3*	*300.2*	*315.3*	*343.0*	*324.5*	*302.4*	*314.1*
Cedex/YSI/pH/HPLC	Pyr	(mg/L)	80.80	82.80	87.70	93.60	87.19	97.17	100.17	83.90	83.68	24.36	24.88	69.82	17.97	55.05	59.58
	Gluc	(g/L)	3.25	3.38	3.21	2.71	2.80	2.79	2.53	2.35	2.29	1.13	1.09	1.11	0.95	0.93	1.00
	Lac	(g/L)	0.588	0.579	0.538	1.15	1.19	1.08	1.61	1.67	1.65	2.80	2.71	2.87	3.06	2.99	3.32
	Gln	(mM)	1.720	1.710	2.110	1.53	1.48	1.48	1.28	1.25	1.21	0.74	0.66	0.75	0.58	0.59	0.68
	Glu	(mM)	0.363	0.374	0.479	0.42	0.40	0.33	0.33	0.34	0.35	0.35	0.37	0.37	0.36	0.33	0.36
	pH		8.00	8.03	8.10	8.06	8.02	8.04	7.84	7.83	7.79	7.04	7.03	7.04	6.88	6.93	6.96
	VCD	(10^5 cells/mL)	5.60	4.74	6.07	12.23	12.32	12.53	18.82	20.16	20.15	38.16	36.24	37.68	38.29	34.96	34.76
	Via	(%)	96.3	97.0	96.2	94.7	96.1	96.8	95.1	95.1	93.5	95.8	95.4	94.5	94.2	94.5	94.0

	20%: Run 1		1-1	1-2	1-3	2-1	2-2	2-3	3-1	3-2	3-3	4-1	4-2	4-3	5-1	5-2	5-3
	Time	(hours)	1410	1410	1410	2380	2380	2380	2835	2835	2835	3500	3500	3500	4265	4265	4265
Nova Bioanalyzer	*pH*		*8.231*	*8.229*	*8.347*	*8.188*	*8.086*	*8.125*	*7.911*	*7.888*	*7.876*	*7.526*	*7.538*	*7.562*	*7.411*	*7.355*	*7.381*
	Gln	*(mM)*	*1.29*	*1.32*	*1.34*	*1.01*	*0.89*	*0.89*	*0.57*	*0.54*	*0.53*	*0.17*	*0.17*	*0.07*	*0.00*	*0.00*	*0.07*
	Glu	*(mM)*	*0.40*	*0.57*	*0.37*	*0.36*	*0.40*	*0.36*	*0.33*	*0.36*	*0.47*	*0.39*	*0.44*	*0.42*	*0.35*	*0.43*	*0.34*
	Gluc	*(g/L)*	*2.57*	*2.78*	*2.52*	*2.06*	*1.81*	*1.96*	*1.39*	*1.43*	*1.57*	*1.02*	*1.05*	*1.08*	*0.80*	*0.94*	*0.94*
	Lac	*(g/L)*	*0.76*	*0.87*	*0.86*	*1.45*	*1.39*	*1.37*	*1.49*	*1.69*	*1.71*	*1.86*	*1.93*	*1.89*	*2.14*	*2.30*	*2.34*
	NH4+	*(mM)*	*0.52*	*0.56*	*0.48*	*0.62*	*0.52*	*0.49*	*0.69*	*0.68*	*0.64*	*1.01*	*0.93*	*1.04*	*1.12*	*1.24*	*1.30*
	Na+	*(mM)*	*109.5*	*117.9*	*105.0*	*124.4*	*108.2*	*114.1*	*100.7*	*113.8*	*119.4*	*117.5*	*118.8*	*120.5*	*131.4*	*143.8*	*147.1*
	K+	*(mM)*	*4.54*	*4.85*	*4.42*	*4.85*	*4.35*	*4.56*	*4.04*	*4.44*	*4.63*	*4.43*	*4.49*	*4.49*	*4.97*	*5.29*	*5.45*
	Osm	*(mOsm/kg)*	*295.8*	*314.4*	*287.9*	*329.1*	*295.8*	*307.7*	*280.4*	*307.9*	*319.6*	*315.0*	*318.3*	*321.4*	*344.4*	*370.4*	*377.4*
Cedex/YSI/pH/HPLC	Pyr	(mg/L)	86.98	78.79	80.74	73.90	71.95	75.01	60.61	60.92	62.66	43.36	21.90	38.98	14.06	12.77	11.36
	Gluc	(g/L)	3.38	3.46	3.55	2.69	2.62	2.74	2.11	2.01	2.11	1.40	1.35	1.33	1.01	1.01	1.03
	Lac	(g/L)	0.697	0.632	0.643	1.58	1.64	1.61	1.93	2.22	2.21	2.76	2.69	2.59	3.13	3.14	3.39
	Gln	(mM)	2.770	2.620	2.120	1.52	1.84	1.33	1.77	1.08	0.84	0.43	0.50	0.58	0.19	0.17	0.27
	Glu	(mM)	0.520	0.458	0.415	0.43	0.44	0.32	0.50	0.33	0.26	0.23	0.43	0.44	0.28	0.40	0.42
	pH		7.92	7.98	8.01	7.78	7.79	7.79	7.86	7.64	7.66	7.37	7.45	7.49	7.32	7.26	7.21
	VCD	(10^5 cells/mL)	9.66	8.89	7.45	28.07	27.64	23.91	35.28	41.04	34.80	61.44	59.20	57.67	59.43	55.88	53.03
	Via	(%)	94.9	94.6	93.5	97.5	97.4	98.6	98.5	98.4	98.4	96.2	95.3	97.5	89.8	91.5	91.3

	0% Run 2		6-1	6-2	6-3	7-1	7-2	7-3	8-1	8-2	8-3	9-1	9-2	9-3	10-1	10-2	10-3
	Time	(hours)	1385	1385	1385	1920	1920	1920	2285	2285	2285	3020	3020	3020	3285	3285	3285
Nova Bioanalyzer	*pH*		*8.211*	*8.289*	*8.280*	*8.180*	*8.234*	*8.207*	*8.191*	*8.235*	*8.203*	*8.034*	*7.956*	*7.873*	*7.710*	*7.633*	*7.652*
	Gln	*(mM)*	*1.56*	*1.56*	*1.53*	*1.55*	*1.55*	*1.49*	*1.46*	*1.65*	*1.45*	*1.35*	*1.46*	*1.38*	*1.43*	*1.38*	*1.32*
	Glu	*(mM)*	*0.34*	*0.37*	*0.38*	*0.42*	*0.36*	*0.36*	*0.34*	*0.39*	*0.37*	*0.39*	*0.42*	*0.43*	*0.46*	*0.40*	*0.39*
	Gluc	*(g/L)*	*2.68*	*2.58*	*2.59*	*2.49*	*2.47*	*2.38*	*2.28*	*2.55*	*2.29*	*1.82*	*2.03*	*1.75*	*1.61*	*1.47*	*1.43*
	Lac	*(g/L)*	*0.96*	*0.93*	*0.90*	*1.14*	*1.11*	*1.11*	*1.22*	*1.26*	*1.21*	*1.56*	*1.68*	*1.68*	*1.88*	*1.82*	*1.83*
	NH4+	*(mM)*	*0.33*	*0.31*	*0.30*	*0.36*	*0.36*	*0.35*	*0.33*	*0.33*	*0.32*	*0.50*	*0.48*	*0.50*	*0.64*	*0.54*	*0.54*
	Na+	*(mM)*	*122.6*	*115.8*	*112.5*	*119.1*	*119.6*	*119.7*	*126.9*	*129.8*	*120.5*	*128.8*	*134.8*	*124.6*	*139.0*	*123.5*	*126.1*
	K+	*(mM)*	*5.06*	*4.84*	*4.75*	*4.96*	*4.97*	*4.98*	*5.19*	*5.26*	*5.01*	*5.24*	*5.41*	*5.13*	*5.50*	*5.08*	*5.16*
	Osm	*(mOsm/kg)*	*323.6*	*309.6*	*303.0*	*317.9*	*318.4*	*318.1*	*332.5*	*340.0*	*320.2*	*337.7*	*351.6*	*330.6*	*359.8*	*328.5*	*333.4*
Cedex/YSI/pH/HPLC	Pyr	(mg/L)	66.34	74.12	73.13	66.13	66.19	66.02	54.59	61.63	53.81	43.47	38.48	37.30	35.74	36.07	36.46
	Gluc	(g/L)	3.46	3.50	3.47	3.18	3.18	3.16	2.99	3.04	3.01	2.15	2.25	2.10	1.70	1.79	1.77
	Lac	(g/L)	0.786	0.700	0.707	1.06	1.06	1.10	1.36	1.26	1.34	2.16	2.09	2.24	2.75	2.62	2.67
	Gln	(mM)	3.390	4.190	3.200	2.54	2.24	1.72	3.42	2.26	2.04	1.64	2.18	1.60	1.38	1.74	1.62
	Glu	(mM)	0.490	0.674	0.471	0.38	0.32	0.23	0.61	0.35	0.33	0.28	0.41	0.28	0.29	0.33	0.33
	pH		7.79	7.91	7.95	7.67	7.77	7.81	7.40	7.63	7.72	7.62	7.56	7.59	7.30	7.30	7.32
	VCD	(10^5 cells/mL)	4.53	3.60	3.99	6.83	7.01	5.52	8.49	6.70	8.11	10.77	10.19	10.33	13.61	13.32	12.84
	Via	(%)	98.8	99.1	99.4	99.2	98.9	99.4	98.2	97.8	97.8	99.0	98.2	97.9	98.1	97.0	95.7

	2% Run 2		6-1	6-2	6-3	7-1	7-2	7-3	8-1	8-2	8-3	9-1	9-2	9-3
	Time	(hours)	1245	1245	1245	1595	1595	1595	1735	1735	1735	1930	1930	1930
Nova Bioanalyzer	*pH*		*8.671*	*8.380*	*8.282*	*8.691*	*8.265*	*8.322*	*8.498*	*8.341*	*8.275*	*8.492*	*8.311*	*8.363*
	Gln	*(mM)*	*1.48*	*1.56*	*1.51*	*1.38*	*1.67*	*1.70*	*1.51*	*1.49*	*1.49*	*1.38*	*1.60*	*1.50*
	Glu	*(mM)*	*0.56*	*0.33*	*0.43*	*0.45*	*0.36*	*0.36*	*0.48*	*0.34*	*0.41*	*0.59*	*0.42*	*0.39*
	Gluc	*(g/L)*	*2.70*	*2.84*	*2.81*	*2.56*	*3.14*	*3.10*	*2.80*	*2.79*	*2.83*	*2.51*	*2.93*	*2.90*
	Lac	*(g/L)*	*0.84*	*0.73*	*0.68*	*0.84*	*0.87*	*0.87*	*0.92*	*0.84*	*0.86*	*1.01*	*0.98*	*0.92*
	NH4+	*(mM)*	*0.35*	*0.30*	*0.31*	*0.35*	*0.37*	*0.29*	*0.38*	*0.34*	*0.40*	*0.44*	*0.40*	*0.36*
	Na+	*(mM)*	*118.1*	*108.3*	*107.4*	*115.9*	*127.9*	*127.3*	*124.5*	*116.3*	*118.3*	*121.8*	*124.9*	*123.0*
	K+	*(mM)*	*4.92*	*4.65*	*4.61*	*4.86*	*5.25*	*5.20*	*5.13*	*4.88*	*4.96*	*5.02*	*5.13*	*5.09*
	Osm	*(mOsm/kg)*	*313.8*	*294.5*	*292.1*	*308.8*	*335.4*	*333.9*	*327.6*	*310.8*	*315.3*	*321.8*	*329.7*	*325.2*
Cedex/YSI/pH/HPLC	Pyr	(mg/L)	84.04	85.69	84.29	84.19	81.71	81.85	84.22	82.34	83.88	80.30	82.25	78.47
	Gluc	(g/L)	3.68	3.69	3.61	3.62	3.53	3.48	3.59	3.54	3 43	3.32	3.26	3.28
	Lac	(g/L)	0.470	0.471	0.461	0.65	0.65	0.63	0.71	0.71	0.69	0.77	0.76	0.78
	Gln	(mM)	1.580	2.390	1.680	1.85	2.57	1.69	1.86	1.66	1.81	2.37	2.26	2.28
	Glu	(mM)	0.188	0.345	0.233	0.29	0.44	0.27	0.29	0.27	0.29	0.42	0.39	0.42
	pH		8.06	8.06	8.00	8.01	8.03	8.05	7.95	8.02	8.05	7.84	7.93	7.97
	VCD	(10^5 cells/mL)	2.94	3.19	2.60	4.34	4.42	4.43	5.39	5.48	5.00	5.85	6.42	6.43
	Via	(%)	97.9	94.9	97.0	97.9	97.7	95.6	97.1	96.4	87.6	86.6	94.8	93.4

	5% Run 2		6-1	6-2	6-3	7-1	7-2	7-3	8-1	8-2	8-3	9-1	9-2	9-3	10-1	10-2	10-3
	Time	(hours)	1520	1520		1915	1915		2595	2595		2990	2990		3240	3240	
Nova Bioanalyzer	*pH*		*8.197*	*8.236*		*8.132*	*8.256*		*8.154*	*8.247*		*8.100*	*8.153*		*8.108*	*8.088*	
	Gln	*(mM)*	*2.08*	*1.59*		*1.76*	*1.54*		*1.38*	*1.45*		*1.21*	*1.17*		*1.09*	*1.10*	
	Glu	*(mM)*	*0.35*	*0.33*		*0.32*	*0.33*		*0.34*	*0.37*		*0.44*	*0.38*		*0.36*	*0.46*	
	Gluc	*(g/L)*	*3.31*	*2.69*		*2.95*	*2.48*		*2.14*	*2.36*		*1.81*	*1.72*		*1.54*	*1.62*	
	Lac	*(g/L)*	*0.81*	*0.69*		*0.93*	*0.84*		*1.36*	*1.49*		*1.84*	*1.81*		*2.14*	*2.25*	
	NH4+	*(mM)*	*0.29*	*0.26*		*0.28*	*0.28*		*0.29*	*0.41*		*0.50*	*0.50*		*0.53*	*0.47*	
	Na+	*(mM)*	*130.7*	*112.3*		*122.4*	*107.5*		*122.9*	*129 0*		*125.8*	*123.0*		*128.9*	*141.9*	
	K+	*(mM)*	*5.27*	*4.66*		*4.99*	*4.50*		*4.92*	*5.11*		*4.93*	*4.86*		*5.01*	*5.44*	
	Osm	*(mOsm/kg)*	*340.8*	*300.6*		*324.2*	*291.9*		*325.3*	*339.8*		*334.6*	*328.4*		*342.4*	*368.9*	
Cedex/YSI/pH/HPLC	Pyr	(mg/L)	77.33	77.60		83.52	81.37		78.51	67.82		65.03	68.37		57.79	62.17	
	Gluc	(g/L)	3.51	3.48		3.30	3.28		2.83	2.62		2.05	2.05		1.76	1.82	
	Lac	(g/L)	0.534	0.537		0.72	0.73		1.43	1.36		1.90	1.97		2.35	2.56	
	Gln	(mM)	2.190	2.290		1.62	2.02		0.75	1.83		1.33	1.81		2.24	1.22	
	Glu	(mM)	0.355	0.383		0.28	0.38		0.15	0.42		0.23	0.20		0.46	0.23	
	pH		7.91	0.00		8.06	7.98		7.76	7.73		7.72	7.63		7.37	7.35	
	VCD	(10^5 cells/mL)	5.59	5.37		8.36	8.35		18.87	18.22		23.38	24.73		30.14	26.73	
	Via	(%)	96.1	97.3		96.7	96.3		97.3	96.9		98.3	98.1		97.5	97.0	

	10% Run 2		6-1	6-2	6-3	7-1	7-2	7-3	8-1	8-2	8-3	9-1	9-2	9-3	10-1	10-2	10-3
	Time	(hours)	1480	1480	1480	1830	1830	1830	2110	2110	2110	2340	2340	2340	2685	2685	2685
Nova Bioanalyzer	*pH*			*8.183*	*8.206*	*8.226*	*8.175*	*8.153*	*8.111*	*8.091*	*8.097*	*7.673*	*8.016*	*7.894*	*7.777*		
	Gln	*(mM)*		*1.82*	*1.78*	*1.59*	*1.55*	*1.56*	*1.37*	*1.50*		*2.25*	*2.33*	*2.61*	*1.85*		
	Glu	*(mM)*		*0.33*	*0.37*	*0.39*	*0.41*	*0.41*	*0.41*	*0.43*							
	Gluc	*(g/L)*		*3.08*	*2.99*	*2.78*	*2.71*	*2.66*	*2.44*	*2.59*		*4.89*	*4.25*	*5.29*	*4.15*		
	Lac	*(g/L)*		*0.97*	*0.98*	*1.23*	*1.20*	*1.20*	*1.36*	*1.58*		*3.39*	*3.31*	*3.54*	*3.84*		
	NH4+	*(mM)*		*0.42*	*0.41*	*0.33*	*0.41*	*0.43*	*0.51*	*0 55*	*0.39*		*0.42*	*0.56*	*0.62*		
	Na+	*(mM)*		*131.8*	*129.0*	*135.1*	*132.5*	*127.1*	*129.5*	*142.4*	*125.7*	*328.9*	*130.8*	*173.5*	*148.4*		
	K+	*(mM)*		*5.25*	*5.19*	*5.32*	*5.26*	*5.05*	*5.09*	*5.46*	*4.85*		*4.88*	*6.23*	*5.30*		
	Osm	*(mOsm/kg)*		*343.6*	*337.8*	*350.9*	*345.4*	*334.7*	*339.9*	*368.0*	*303.5*		*373.5*	*464.0*	*412.7*		
Cedex/YSI/pH/HPLC	Pyr	(mg/L)		74.51	74.79	67.52	66.65	68.88	72.26	74.08	71.92	63.42	66.94	63.58	49.55	49.58	52.31
	Gluc	(g/L)		3.73	3.77	3.15	3.18	3.34	2.67	2.65	2.72	2.34	2.41	2.36	1 89	1.82	1.86
	Lac	(g/L)		0.813	0.808	1.13	1.10	1.16	1.26	1.39	1.25	1.55	1.48	1.49	2.02	1.97	2.06
	Gln	(mM)		1.680	1.560	1.65	1.50	1.44	1.29	1.45	1.41	1.26	1.41	1.24	0.94	0.97	1.00
	Glu	(mM)		0.215	0.224	0.29	0.26	0.23	0.23	0.30	0.29	0.29	0.32	0.28	0.26	0.28	0.28
	pH			7.72	7.86	0.00	7.93	7.88	7.78	7.77	7.79	7.84	7.82	7.80	7.44	7.44	7.47
	VCD	(10^5 cells/mL)		10.43	10.85	15.64	15.89	13.03	20.14	20.98	20.65	22.52	21.27	22.08	34.19	35.46	33.88
	Via	(%)		97.9	98.2	97.9	98.2	97.5	98.6	98.4	98.3	98.3	97.8	97.8	98.4	98.9	98.0

	20% Run 2		6-1	6-2	6-3	7-1	7-2	7-3	8-1	8-2	8-3	9-1	9-2	9-3	10-1	10-2	10-3
	Time	(hours)	1620	1620	1620	1860	1860	1860	2045	2045	2045	2215	2215	2215	2590	2590	2590
Nova Bioanalyzer	*pH*		*8.197*	*8.236*	*8.198*	*8.132*	*8.256*	*8.145*	*8.154*	*8.247*	*8.237*	*8.100*	*8.153*	*8.207*	*8.108*	*8.088*	*8.055*
	Gln	*(mM)*	*1.41*	*1.51*	*1.43*	*1.34*	*1.35*	*1.49*	*1.34*	*1.44*	*1.49*	*1.18*	*1.27*	*1.27*	*1.19*	*1.23*	*1.24*
	Glu	*(mM)*	*0.32*	*0.42*	*0.36*	*0.40*	*0.36*	*0.42*	*0.33*	*0.37*	*0.49*	*0.42*	*0.45*	*0.46*	*0.41*	*0.45*	*0.46*
	Gluc	*(g/L)*	*2.56*	*2.77*	*2.57*	*2.41*	*2.48*	*2.67*	*2.33*	*2.63*	*2.75*	*2.21*	*2.25*	*2.63*	*2.27*	*2.48*	*2.40*
	Lac	*(g/L)*	*0.93*	*0.97*	*0.90*	*0.96*	*0.97*	*1.02*	*1.05*	*1.09*	*1.21*	*1.08*	*1.15*	*1.17*	*1.41*	*1.44*	*1.45*
	NH4+	*(mM)*	*0.33*	*0.40*	*0.34*	*0.46*	*0.43*	*0.49*	*0.45*	*0.46*	*0.52*	*0.54*	*0.53*	*0.54*	*0.59*	*0.52*	*0.58*
	Na+	*(mM)*	*111.5*	*122.3*	*116.5*	*115.7*	*116.1*	*127.2*	*115.4*	*126.5*	*137.3*	*114.6*	*116.1*	*136.4*	*137.9*	*150.5*	*149.7*
	K+	*(mM)*	*4.66*	*4.98*	*4.82*	*4.79*	*4.83*	*5.14*	*4.76*	*5.08*	*5.42*	*4.78*	*4.80*	*5.38*	*5.35*	*5.75*	*5.69*
	Osm	*(mOsm/kg)*	*301.2*	*323.6*	*310.5*	*309.0*	*310.3*	*333.2*	*308.9*	*332.3*	*355.1*	*307.3*	*311.1*	*352.3*	*355.8*	*381.3*	*379.5*
Cedex/YSI/pH/HPLC	Pyr	(mg/L)	85.39	77.03	77.84	77.65	77.77	76.25	77.55	74.90	75.19	77.76	75.28	75.32	77.04	81.76	83.64
	Gluc	(g/L)	3.40	3.28	3.39	3.31	3.25	3.21	3.20	3.11	3.14	3.10	3.06	2.99	2.71	2.88	2.74
	Lac	(g/L)	0.699	0.690	0.671	0.83	0.82	0.78	0.97	0.92	0.96	1.12	1.08	1.03	1.48	1.52	1.45
	Gln	(mM)	2.080	1.880	2.010	2.10	2.59	1.79	2.07	1.87	1.73	1.90	1.51	2.09	2.01	1.35	1.97
	Glu	(mM)	0.249	0.320	0.275	0.37	0.42	0.44	0.47	0.35	0.39	0.36	0.23	0.44	0.50	0.29	0.56
	pH		7.83	7.85	7.86	8.03	7.97	7.96	7.80	7.80	7.90	7.87	7.91	7.91	7.82	7.76	7.80
	VCD	(10^5 cells/mL)	9.33	12.18	10.71	12.21	12.59	12.43	14.45	14.31	14.40	15.90	17.11	17.29	21.63	22.12	23.38
	Via	(%)	96.1	97.2	96.2	97.2	97.5	96.5	98.2	97.3	98.0	97.2	96.8	97.0	97.8	97.6	97.6

REFERENCES

Adelman, D. M., M. Gertsenstein, A. Naggy, M. C. Simon, and E. Maltepe. (2000). Placental cell fates are regulated *in vivo* by HIF-mediated hypoxia responses. *Genes and Development 14*:3191-3203.

Bradley, A., M. Evans, M. Kaufman, and E. Robertson. (1984). Formation of germ-line chimaeras from embryo-derived teratocarcinoma cell lines. *Nature 309*:255-56.

Caniggia, I., H. Mostachfi, J. Winter, M. Gassmann, S. J. Lye, M. Kuliszewski, and M. Post. (2000). Hypoxia-inducible factor-1 mediates the biological effects of oxygen on human trophoblast differentiation through $TGF\beta_3$. *The Journal of Clinical Investigation 105*:577-587.

Carmeliet, P., Y. Dor, J. M. Herbert, D. Fukumura, K. Brusselmans, M. Dewerchin, M. neeman, F. Bono, R. Abramovitch, P. Maxwell, C. J. Koch, P. Ratcliffe, L. Moons, R. K. Jain, D. Collen, E. Keshet. (1998). Role of HIF-1a in hypoxia-mediated apoptosis, cell proliferation and tumor angiogenesis. *Nature 394*:485-490.

Cruz, H. J., J. L. Moreira and M. J. T. Carrondo. (1999). Metabolic Shifts by Nutrient Manipulation in Continuous Cultures of BHK Cells. *Biotechnology and Bioengineering 66*(2):104-113.

Cruz, H. J., C. M. Freitas, P. M. Alves, J. L. Moreira, and M. J. T. Carrondo. (2000). Effects of ammonia and lactate on growth, metabolism, and productivity of BHK cells. *Enzyme and Microbial Technology 27*:43-52.

Europa, A. F., A. Gambhir, P. Fu, and W. Hu. (2000). Multiple steady states with distinct cellular metabolism in continuous culture of mammalian cells. *Biotechnology and Bioengineering 67*(1):25-34.

Evans, M. J. and M. H. Kaufman. (1981). Establishment in culture of pluripotential cells from mouse embryos. *Nature 292*:154-156.

Fischer, B. and B. D. Bavister. (1993). Oxygen tension in the oviduct and uterus of rhesus monkeys, hamsters, and rabbits. *Journal of Reproduction and Fertility. 99(2)*:673-9.

Gassmann, M., J. Fandrey, S. Bichet, M. Wartenberg, H. H. Marti, C. Bauer, R. H. Wenger, and H. Acker. (1996). Oxygen supply and oxygen-dependent gene expression in differentiating embryonic stem cells. *Proceedings of the National Academy of Science (USA) 93*:2867-2872.

Gilbert, S. F. (1997). *Developmental Biology.* Sunderland, Massachusetts: Sinauer Associates, Inc.

Gstraunthaler, Gerhard, Thomas Seppi, and Walter Pfaller. (1999). Impact of Culture Conditions, Culture Media Volumes, and Glucose Content on Metabolic Properties of Renal Epithelial Cell Cultures. *Cellular Physiology and Biochemistry 9*:150-172.

Iyer, N. V., L. E. Kotch, F. Agani, S. W. Leung, E. Laughner, R. H. Wenger, M. Gassmann, J. D. Gearhart, A. M. Lawler AM, A. Y. Yu, and G. L. Semenza (1998). Cellular and developmental control of O_2 homeostasis by hypoxia-inducible factor 1α. *Genes and Development 12*:149-162.

Jang, J. D. and J. P. Barford. (2000). An unstructured kinetic model of macromolecular metabolism in batch and fed-batch cultures of hybridoma cells producing monoclonal antibody. *Biochemical Engineering Journal 4*:153-168.

Lao, M. and D. Toth. (1997). Effects of Ammonium and Lactate on Growth and Metabolism of a Recombinant Chinese Hamster Ovary Cell Culture. *Biotechnology Progress 13*:688-691.

Linz, M., A. Zeng, R. Wagner, and W. Deckwer. (1997). Stoichiometry, Kinetics, and Regulation of Glucose and Amino Acid Metabolism of a BHK Cell Line in Batch and Continuous Cultures. *Biotechnology Progress 13*:453-463.

Ljunggren, J. and L Häggström. (1995). Specific growth rate as a parameter for tracing growth-limiting substances in animal cell cultures. *Journal of Biotechnology 42*:163-175.

Martin, G. R. (1981). Isolation of a Pluripotent Cell Line from Early Mouse Embryos Cultured in Medium Conditioned by Teratocarcinoma Stem Cells. *Proceedings of the National Academy of Science (USA) 78*:7634-7638.

Nelson, D. L. and M. M. Cox. (2000). *Lehninger Principles of Biochemistry.* New York: Worth Publishers.

Nichols, J. (2001) Introducing embryonic stem cells. *Current Biology 11*(13):R503-R505.

Noda, Y., H. Matsumoto, Y. Umaoka, K. Tatsumi, J. Kishi, and T. Mori. (1991). Involvement of superoxide radicals in the mouse two-cell block. *Molecular Reproduction and Development 28*(4):256-60.

Orsi, N. M. and H. J. Leese. (2001). Protection Against Reactive Oxygen Species During Mouse Preimplantation Embryo Development: Role of EDTA, Oxygen Tension, Catalase, Superoxide Dismutase and Pyruvate. *Molecular Reproduction and Development. 59*:44-53.

Ozturk, S. S. and B.O. Palsson. (1990). Effects of Dissolved Oxygen on Hybridoma Cell Growth, Metabolism, and Antibody Production Kinetics in Continuous Culture. *Biotechnology Progress 6*:437-446.

Petch, D. and M. Butler. (1994). Profile of energy metabolism in a murine hybridoma: glucose and glutamine utilization. *Journal of Cellular Physiology 161*:71-76.

Potter, S. M. and T. B. DeMarse. (2001). A new approach to neural cell culture for long-term studies. *Journal of Neuroscience Methods 110*(1-2):17-24.

Potocnik, A. J., P. J. Nielsen, and K. Eichmann. (1994). *In vitro* generation of lymphoid precursors from embryonic stem cells. *The EMBO Journal 13*(22):5274-5283.

Quinn, P. and G. M. Harlow. (1978). The effect of oxygen on the development of preimplantation mouse embryos *in vitro*. *Journal of Experimental Zoology 206*(1):73-80.

Sanford, K. K., B. B. Westfall, and J. L. Jackson. (1970). Glycolysis during culture of neoplastic and non-neoplastic murine cell lines under aerobic and anaerobic conditions. *Journal of the National Cancer Institute 44*(3):611-614.

Savatier, P., H. Lapillonne, L. A. van Grunsven, B. B. Rudkin, and J Samarut. (1995). Withdrawal of differentiation inhibitory activity/leukemia inhibitory factor up-regulates D-type cyclins and cyclin-dependent kinase inhibitors in mouse embryonic stem cells. *Oncogene 12*:309-322.

Silverman, H. S., S. Wei, M. C. P. Haigney, C. J. Ocampo, and M. D. Stern. (1997). Myocyte adaptation to chronic hypoxia and development of tolerance to subsequent acute severe hypoxia. *Circulation Research 80*:699-707.

Smith, A. G. (2001). Embryo-Derived Stem Cells: Of Mice and Men. *Annual Review of Cellular and Developmental Biology 17*:435-62.

Stem Cells: Scientific Progress and Future Research Directions. Department of Health and Human Services. June 2001. http://www.nih.gov/news/stemcell/scireport.htm

Taylor, John R. (1997). *An Introduction to Error Analysis.* Sausalito, CA: University Science Books

Wang, M. D., M. Yang, N. Huzel, and M. Butler. (2002). Erythropoietin Production from CHO Cells Grown by Continuous Culture in a Fluidized Bed Bioreactor. *Biotechnology and Bioengineering 77*:194-203.

Wiles, M. V. (1993). Embryonic Stem Cell Differentiation *in vitro*. *Methods in Enzymology 225*:900-918.

Williams, R. L., et. al. (1988). Myeloid leukaemia inhibitory factor maintains the developmental potential of embryonic stem cells. *Nature 336*(6200): 684-7.

Wobus, A. M. (2001). Potential of embryonic stem cells. *Molecular Aspects of Medicine 22*:149-164.

Yochim, J.M. and J. A. Michell. Intrauterine Oxygen Tension in the Rat During Progestation: Its Possible Relation to Carbohydrate Metabolism and the Regulation of Nidation. *Endocrinology 83*:706-713.

Zandstra, P.W. and A. Nagy. Stem Cell Bioengineering. *Annual Review of Biomedical Engineering 2001 3*:275-305.

Zar, Jerold H. (1996) *Biostatistical Analysis.* Upper Saddle River, NJ: Prentice Hall.

Zielke, H. Ronald, Carlota M. Sumbilla, David A. Sevdalian, Robert L. Hawkins, and Pinar T. Ozand. (1980). Lactate: a major product of glutamine metabolism by human diploid fibroblasts. *Journal of Cellular Physiology 104*(3):433-41.

Zielke, H. Ronald, Carol L. Zielke, and Pinar T. Ozand. (1984). Glutamine: a major energy source for cultured mammalian cells. *Federation Proceedings 43*(1):121-125.

Zhou, W., J. Rehm, A. Europa, and W. Hu. (1997). Alteration of mammalian cell metabolism by dynamic nutrient feeding. *Cytotechnology 24*:99-108.